

# Insight into the Efficiency of Cinnamyl-Supported Precatalysts for the Suzuki–Miyaura Reaction: Observation of Pd(I) Dimers with Bridging Allyl Ligands During Catalysis

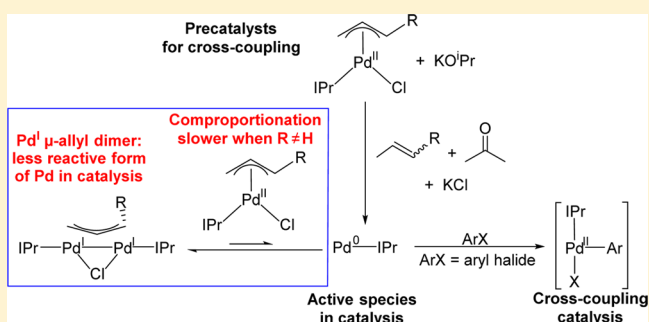
Damian P. Hruszkewycz,<sup>†</sup> David Balcells,<sup>\*,‡</sup> Louise M. Guard,<sup>†</sup> Nilay Hazari,<sup>\*,†</sup> and Mats Tilset<sup>‡</sup>

<sup>†</sup>The Department of Chemistry, Yale University, P.O. Box 208107, New Haven, Connecticut 06520, United States

<sup>‡</sup>Centre for Theoretical and Computational Chemistry (CTCC), Department of Chemistry, University of Oslo, P.O. Box 1033 Blindern, 0315 Oslo, Norway

**S** Supporting Information

**ABSTRACT:** Despite widespread use of complexes of the type Pd(L)( $\eta^3$ -allyl)Cl as precatalysts for cross-coupling, the chemistry of related Pd<sup>I</sup> dimers of the form ( $\mu$ -allyl)( $\mu$ -Cl)Pd<sub>2</sub>(L)<sub>2</sub> has been underexplored. Here, the relationship between the monomeric and the dimeric compounds is investigated using both experiment and theory. We report an efficient synthesis of the Pd<sup>I</sup> dimers ( $\mu$ -allyl)( $\mu$ -Cl)Pd<sub>2</sub>(IPr)<sub>2</sub> (allyl = allyl, crotyl, cinnamyl; IPr = 1,3-bis(2,6-diisopropylphenyl)imidazol-2-ylidene) through activation of Pd(IPr)( $\eta^3$ -allyl)Cl type monomers under mildly basic reaction conditions. The catalytic performance of the Pd<sup>II</sup> monomers and their Pd<sup>I</sup>  $\mu$ -allyl dimer congeners for the Suzuki–Miyaura reaction is compared. We propose that the ( $\mu$ -allyl)( $\mu$ -Cl)Pd<sub>2</sub>(IPr)<sub>2</sub>-type dimers are activated for catalysis through disproportionation to Pd(IPr)( $\eta^3$ -allyl)Cl and monoligated IPr–Pd<sup>0</sup>. The microscopic reverse comproportionation reaction of monomers of the type Pd(IPr)( $\eta^3$ -allyl)Cl with IPr–Pd<sup>0</sup> to form Pd<sup>I</sup> dimers is also studied. It is demonstrated that this is a facile process, and Pd<sup>I</sup> dimers are directly observed during catalysis in reactions using Pd<sup>II</sup> precatalysts. In these catalytic reactions, Pd<sup>I</sup>  $\mu$ -allyl dimer formation is a deleterious process which removes the IPr–Pd<sup>0</sup> active species from the reaction mixture. However, increased sterics at the 1-position of the allyl ligand in the Pd(IPr)( $\eta^3$ -crotyl)Cl and Pd(IPr)( $\eta^3$ -cinnamyl)Cl precatalysts results in a larger kinetic barrier to comproportionation, which allows more of the active IPr–Pd<sup>0</sup> catalyst to enter the catalytic cycle when these substituted precatalysts are used. Furthermore, we have developed reaction conditions for the Suzuki–Miyaura reaction using Pd(IPr)( $\eta^3$ -cinnamyl)Cl which are compatible with mild bases.



## INTRODUCTION

Pd-catalyzed cross-coupling is an area of intense research interest because it has numerous applications in the synthesis of pharmaceuticals, fine chemicals, and materials.<sup>1</sup> In the last 20 years one of the major advances in the field has been the development of specialized phosphine- and NHC-based ligands, such as those designed by Fu,<sup>2</sup> Buchwald,<sup>3</sup> Hartwig,<sup>4</sup> and Stradiotto,<sup>5</sup> which promote many of the fundamental steps in catalysis such as oxidative addition and reductive elimination.<sup>1g,h</sup> Use of these relatively new ligands has resulted in an expanded substrate scope, milder reaction conditions, and lower catalyst loadings.<sup>1g,h</sup> Unfortunately, these specialized ligands often have comparable expense to the Pd source, which means that the traditional route for generating the Pd<sup>0</sup> active species, addition of excess ligand to a Pd<sup>0</sup> or Pd<sup>II</sup> precursor, is not always attractive. Furthermore, in many cases it has been determined that the optimal Pd to ligand ratio is 1:1 and that the active species is monoligated L–Pd<sup>0</sup>.<sup>6</sup> As a result, a number of well-defined Pd<sup>II</sup> precatalysts with a 1:1 Pd to ligand ratio, such as Buchwald's palladacycles,<sup>7</sup> Organ's PEPPSI complexes,<sup>8</sup>

and Nolan's allyl-based systems<sup>9</sup> (Figure 1), have been developed and are now commercially available.

A key feature in determining the effectiveness of these precatalysts is the rate and efficiency of their conversion into the monoligated L–Pd<sup>0</sup> active species under the reaction conditions.<sup>1c,hi</sup> Extensive studies have been performed on the mechanism of activation of the Buchwald<sup>7b</sup> and Organ

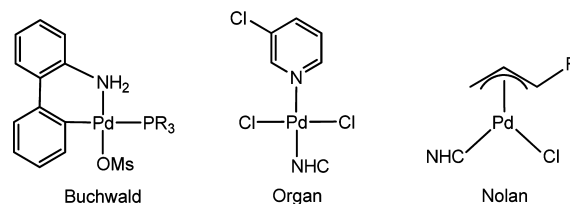


**Figure 1.** Three popular well-defined precatalyst scaffolds with a 1:1 Pd to ligand ratio.

Received: December 10, 2013

Published: April 24, 2014

**Scheme 1.** Two Steps Which Are Proposed to Be Relevant to Activation of Allyl-Containing Precatalysts: (a) Conversion of Pd<sup>II</sup> to Pd<sup>0</sup> and (b) Comproportionation of Pd<sup>0</sup> with Pd<sup>II</sup> to Generate Pd<sup>I</sup>

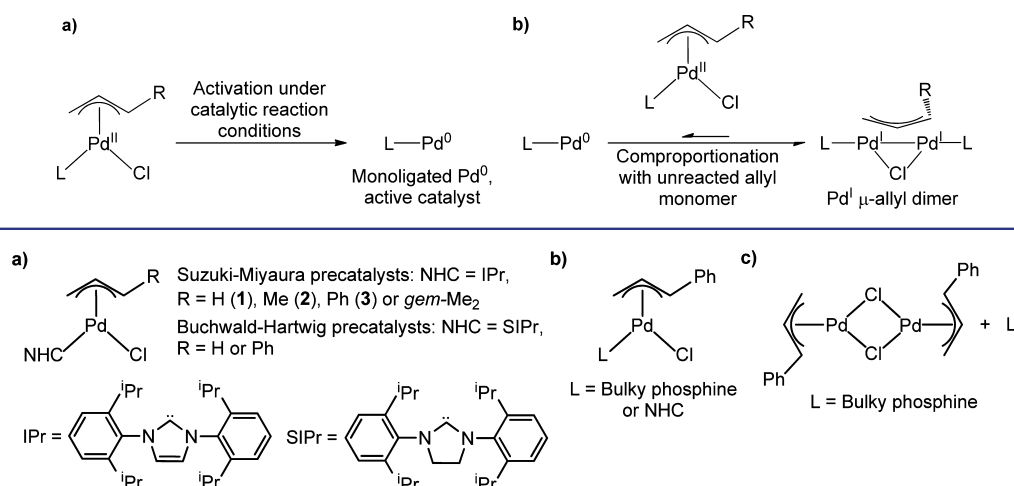
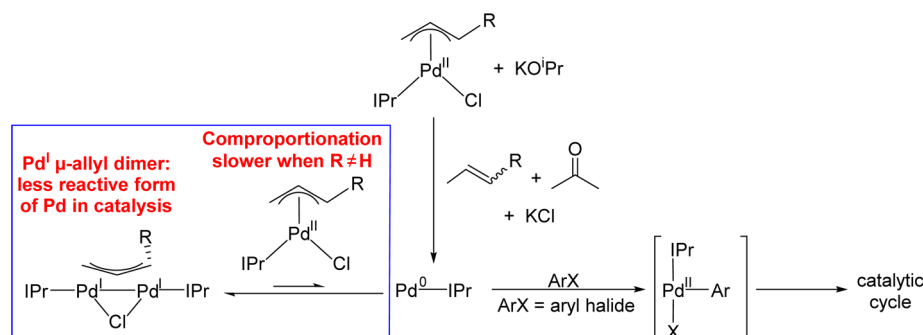


**Figure 2.** (a) Summary of allyl-based precatalysts reported by Nolan and co-workers. (b) Generic structure of cinnamyl-supported Pd<sup>II</sup> precatalysts that are often used in cross-coupling. (c) Dimeric precursor which is often combined with a bulky ligand in situ in cross-coupling.

**Scheme 2.** Our Proposed Pathway for Activation of Precatalysts of the Type Pd(IPr)(η<sup>3</sup>-allyl)Cl<sup>a</sup>



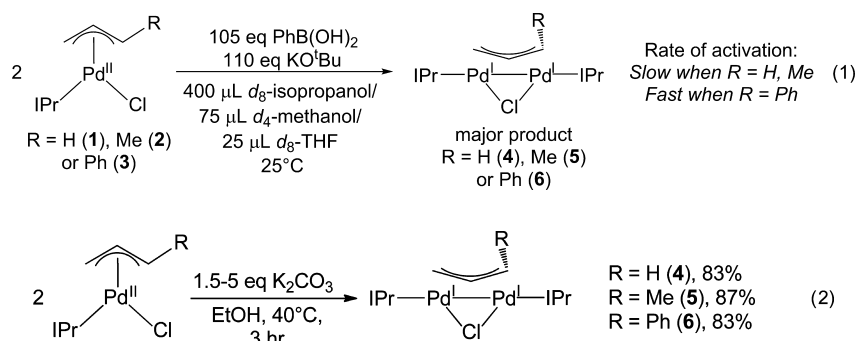
<sup>a</sup>Both the rates of activation to Pd<sup>0</sup> and comproportionation to Pd<sup>I</sup> affect overall catalytic activity.

precatalysts,<sup>8b,10</sup> and these activation pathways are now relatively well understood. In contrast, relatively little is known about the mechanism of activation of allyl-based precatalysts. It is proposed that activation of these species can be split into two steps (Scheme 1):<sup>11</sup> (a) activation of the ligated precatalyst scaffold to form the catalytically active monoligated L–Pd<sup>0</sup> species<sup>6</sup> and (b) comproportionation, which forms a Pd<sup>I</sup> μ-allyl dimer<sup>12</sup> and removes the L–Pd<sup>0</sup> from the reaction mixture. Preliminary studies on activation<sup>9b,13</sup> and comproportionation<sup>11</sup> have been reported, but both need to be understood in greater detail. This current work investigates both steps shown in Scheme 1, with an emphasis on b.<sup>14</sup>

To perform these studies we revisit precatalysts of the type Pd(NHC)(η<sup>3</sup>-allyl)Cl (NHC = IPr or SIPr),<sup>9</sup> which were originally reported by Nolan and co-workers in 2002.<sup>9a,b</sup> Subsequently, Nolan demonstrated that addition of substituents in the 1-position of the allyl ligand results in a dramatic improvement in catalytic efficiency for the Suzuki–Miyaura and Buchwald–Hartwig reactions compared to unsubstituted allyl precatalysts.<sup>9d,15</sup> This work has led to the widespread use of complexes of the type Pd(NHC)(η<sup>3</sup>-cinnamyl)Cl (NHC = IPr or SIPr) as precatalysts for both cross-coupling and related reactions<sup>16</sup> and the general use of cinnamyl-supported Pd complexes with other bulky ligands in the cross-coupling literature (Figure 2b).<sup>17</sup> In fact, based on these results the

dimeric precursor (η<sup>3</sup>-cinnamyl)<sub>2</sub>(μ-Cl)<sub>2</sub>Pd<sub>2</sub>, in conjunction with an appropriate ligand, is also extensively used in cross-coupling reactions (Figure 2c).<sup>18</sup> Nolan postulated that the substitution on the allyl ligand weakens bonding between the Pd and the allyl moiety and makes activation to the catalytically active IPr–Pd<sup>0</sup> more facile,<sup>9d</sup> but the precise reason for this enhanced rate of activation and the more efficient performance of cinnamyl-supported species is still unclear. In this contribution, we provide insight into the efficiency of the cinnamyl-supported precatalyst 3. It is demonstrated that Pd<sup>I</sup> μ-allyl dimers of the type (μ-allyl)(μ-Cl)Pd<sub>2</sub>(IPr)<sub>2</sub> form via comproportionation between the corresponding Pd(IPr)(η<sup>3</sup>-allyl)Cl monomers and IPr–Pd<sup>0</sup> in Suzuki–Miyaura reactions that use the monomeric precatalysts (Scheme 1b). The presence of substituents in the 1-position of the allyl ligand raises the kinetic barrier to comproportionation, thus increasing the concentration of the monoligated active catalyst that can enter the catalytic cycle via oxidative addition with the aryl halide substrate (Scheme 2).

Surprisingly, despite the close relationship between complexes of the type Pd(L)(η<sup>3</sup>-allyl)Cl and their Pd<sup>I</sup> μ-allyl dimers analogues little has been done to compare these systems or study the reactivity of Pd<sup>I</sup> μ-allyl dimers.<sup>11a,19</sup> This is even more noteworthy given that in recent years binuclear Pd<sup>I</sup>–Pd<sup>I</sup> complexes have repeatedly been isolated from reaction mixtures



previously thought to involve complexes only in the Pd<sup>0</sup> and Pd<sup>II</sup> oxidation states.<sup>11,19,20</sup> Furthermore, several binuclear Pd<sup>I</sup>–Pd<sup>I</sup> complexes,<sup>21</sup> including Pd<sup>I</sup>  $\mu$ -allyl dimers,<sup>11a,19,22</sup> have been shown to be effective precatalysts for Pd-catalyzed cross-coupling, and their mechanisms of activation have been a topic of ongoing research.<sup>21d,23</sup> In this work, we conduct a detailed comparison of the catalytic efficiency of a series of precatalysts of the type Pd(IPr)( $\eta^3$ -allyl)Cl and their Pd<sup>I</sup>  $\mu$ -allyl dimer analogues for a simple Suzuki–Miyaura reaction. We propose that the Pd<sup>I</sup>  $\mu$ -allyl dimers access the catalytically active IPr–Pd<sup>0</sup> via disproportionation, and we present a detailed study of the disproportionation pathway (Scheme 1b). In addition, through our studies of the synthesis of Pd<sup>I</sup>  $\mu$ -allyl dimers we have discovered a mild way to activate the Pd(NHC)( $\eta^3$ -allyl)Cl scaffold (Scheme 1a) and describe reaction conditions for the Suzuki–Miyaura reaction using precatalysts of the type Pd(L)( $\eta^3$ -allyl)Cl with milder bases.

## RESULTS AND DISCUSSION

**Activation of Pd(IPr)( $\eta^3$ -allyl)Cl.** Although it has previously been postulated that complexes with 1-substituted allyl ligands are activated faster in complexes of the type Pd(IPr)( $\eta^3$ -allyl)Cl,<sup>9d</sup> there is no direct experimental evidence to support this claim. Therefore, our mechanistic investigation began with a study of the activation of 1–3 with excess KO<sup>t</sup>Bu and PhB(OH)<sub>2</sub> at 25 °C (eq 1). The reaction conditions used for these experiments correspond closely to the conditions used for the Suzuki–Miyaura coupling (*vide infra*), but the aryl halide substrate is absent. A mixed solvent system was used to ensure that the reaction was homogeneous, which allows for a more exact comparison of rates. We were surprised that all three monomeric precatalysts formed their corresponding Pd<sup>I</sup>  $\mu$ -allyl dimer as the major product, as determined by <sup>1</sup>H NMR spectroscopy (*vide infra* for characterization of 4–6).<sup>24</sup> However, a large difference in rate was observed between the systems, with 3 being activated completely in less than 5 min, while after 1 h 50–60% of 1 or 2 was still present in solution, and complete conversion was only observed after heating for an additional hour at 40 °C.<sup>24</sup> These results suggest that it is plausible that Pd<sup>I</sup>  $\mu$ -allyl dimers play a role in cross-coupling and that under these conditions the speed of activation never becomes sufficiently fast to prevent dimer formation, presumably through comproportionation between the starting complex of the type Pd(IPr)( $\eta^3$ -allyl)Cl and monoligated IPr–Pd<sup>0</sup> (*vide infra*).

**Synthesis and Characterization of Pd<sup>I</sup>  $\mu$ -Allyl Dimers.** To probe the role of dimers further, we synthesized the IPr-supported Pd<sup>I</sup>  $\mu$ -allyl dimer congeners to Nolan's monomeric species through the reaction of 1–3 with a slight excess of K<sub>2</sub>CO<sub>3</sub> in warm ethanol (eq 2). Excellent yields were obtained

for all of the isolated Pd<sup>I</sup>  $\mu$ -allyl dimers. Complexes 5 and 6 are rare examples of Pd<sup>I</sup>  $\mu$ -allyl dimers with 1-substituted  $\mu$ -allyl ligands.<sup>20d,e,25</sup> Consistent with literature precedent, the  $\mu$ -allyl ligands in the thermodynamically preferred isomers of both 5 and 6 exhibit an *anti* geometry,<sup>25</sup> where the 1-substituent is on the opposite side of the allyl ligand to the central proton, as determined from NOE experiments. In the reaction to form 5, a mixture of *syn* and *anti* isomers is initially formed, which equilibrates almost exclusively to the *anti* isomer (the thermodynamic product) when 5 is left in solution for 48 h at room temperature.<sup>24</sup> In contrast, in the reaction to form 6 only the *anti* isomer is observed under our standard synthetic conditions.<sup>24</sup> The  $\mu$ -allyl ligands in 4, 5, and 6 exhibit distinct <sup>1</sup>H NMR features compared to their monomeric  $\eta^3$ -allyl counterparts.<sup>9b,d</sup> In all three cases the *anti* protons of the  $\mu$ -allyl ligands resonate at abnormally low chemical shifts, in the range of 0.5–0.9 ppm, and the *anti* methyl and phenyl resonances of 5 and 6 are also shifted upfield. The central protons of monomeric  $\eta^3$ -allyl ligands exhibit a chemical shift in the olefinic region,<sup>9b,d</sup> whereas the signals corresponding to the central protons of 4, 5, and 6 are observed between 1.55 and 1.75 ppm. These abnormally low chemical shifts may result in part from the significant electron density present on the  $\mu$ -allyl ligand due to back-bonding from the Pd–Pd bond into the  $\pi^*$  orbital of the  $\mu$ -allyl ligands, an interaction first proposed by Kurosawa and co-workers.<sup>25b,26</sup>

Compounds 5 (Figure 3) and 6 (Figure 4) were characterized by X-ray crystallography. They exhibit similar structural characteristics to 4 and other Pd<sup>I</sup>  $\mu$ -allyl dimers which also contain a  $\mu$ -chloride ligand.<sup>11a,19,27</sup> Consistent with analogous structures, the central carbon atoms of the  $\mu$ -allyl ligands interact with both Pd centers (Pd–C<sub>cent</sub> 2.34–2.39 Å), while the terminal carbon atoms only interact with one Pd atom. Crystallographic analysis suggests that the Pd–C bond distances to the terminal carbon atoms of the  $\mu$ -allyl ligands are not equivalent, although due to disorder this cannot be concluded with absolute certainty.<sup>28</sup> Longer Pd–C bond distances are observed for the carbon atoms, which are attached to either the Me (5) or the Ph (6) substituents. Nolan previously observed a similar Pd–C elongation in the  $\eta^3$ -cinnamyl ligand in the monomeric species 3.<sup>9d</sup> A feature of the structures of 5 and 6 is that the central carbon atoms of the  $\mu$ -allyl ligands are canted toward the Pd–Pd–Cl plane (Figure 5a,  $\theta = 69.3^\circ$  in 5 and  $74.1^\circ$  in 6), whereas in monomeric complexes with  $\eta^3$ -allyl ligands the central carbon is canted away from the L–Pd–Cl plane (Figure 5b).<sup>29</sup> Kurosawa and co-workers previously observed this structural feature in related  $\mu$ -allyl dimers and propose that it is due to back-bonding from the filled d orbitals of the Pd–Pd bond into the empty  $\pi^*$  orbital of the  $\mu$ -allyl ligand.<sup>25b,26</sup> Another noteworthy character-

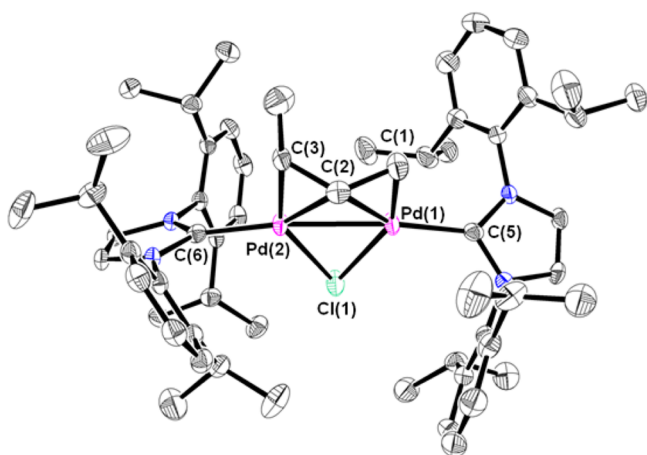


**Figure 3.** ORTEP of **5** (hydrogen atoms have been omitted for clarity). The crotyl fragment crystallized in two conformations, and the major one is shown. Selected bond lengths (Angstroms) and angles (degrees): Pd(1)–Pd(2) 2.5814(7), Pd(1)–C(1) 2.05(2), Pd(1)–C(2) 2.34(1), Pd(2)–C(2) 2.37(2), Pd(2)–C(3) 2.11(2), Pd(1)–Cl(1) 2.433(1), Pd(2)–Cl(1) 2.4368(8), Pd(1)–C(5) 2.013(4), Pd(2)–C(6) 2.017(3), Pd(1)–Pd(2)–C(6) 166.86(8), C(5)–Pd(1)–Pd(2) 164.9(1).

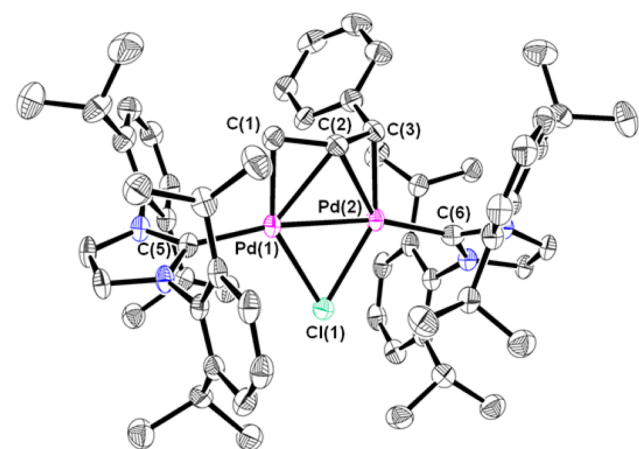


**Figure 4.** ORTEP of **6** (hydrogen atoms have been omitted for clarity). The cinnamyl fragment crystallized in two conformations, and the major one is shown. Selected bond lengths (Angstroms) and angles (degrees): Pd(1)–Pd(2) 2.5999(7), Pd(1)–C(1) 2.04(1), Pd(1)–C(2) 2.390(7), Pd(2)–C(2) 2.377(7), Pd(2)–C(3) 2.09(1), Pd(1)–Cl(1) 2.421(1), Pd(2)–Cl(1) 2.422(1), Pd(1)–C(5) 2.017(5), Pd(2)–C(6) 2.024(5), Pd(1)–Pd(2)–C(6) 166.2(2), C(5)–Pd(1)–Pd(2) 168.0(2).

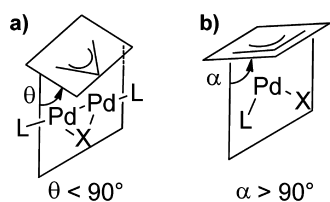


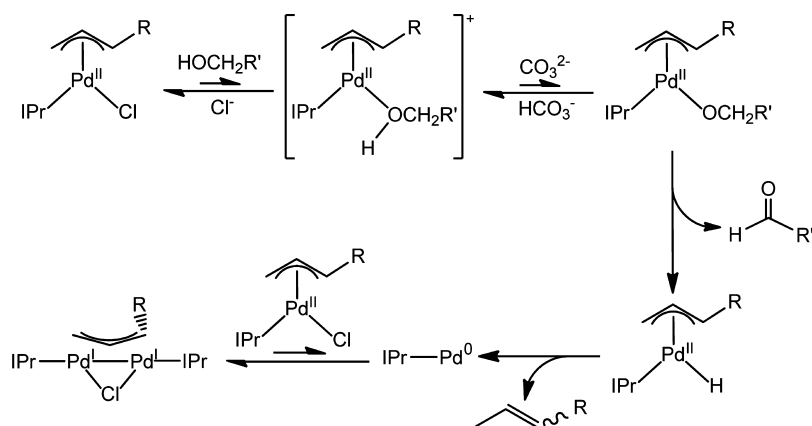
**Figure 5.** Different orientations of the central carbon atoms of the allyl ligand with respect to the Pd bonding planes in (a)  $\mu$ -allyl and (b)  $\eta^3$ -allyl ligands. X is a generic anionic ligand such as Cl.

istic that **5** and **6** share with similar compounds is that the Pd–Pd–IPr angles are not linear.<sup>27,30</sup> Instead, the IPr ligands are oriented away from the central carbon atoms of the  $\mu$ -allyl

ligands, so that the Pd–Pd–IPr angles are between 164° and 169°.

Our new synthetic route for preparation of Pd<sup>I</sup>  $\mu$ -allyl dimers is a vast improvement on previous methods,<sup>27,30</sup> which required formation of air- and moisture-sensitive intermediates. A proposed mechanism for dimer formation is depicted in Scheme 3.<sup>31</sup> The primary alcohol first displaces the chloride ligand. This acidifies the hydroxyl group, which is deprotonated by the weak carbonate base. The resultant Pd<sup>II</sup> alkoxide species is then reduced to a monoligated IPr–Pd<sup>0</sup> complex via  $\beta$ -hydride elimination and reductive elimination of an olefin. Finally, the IPr–Pd<sup>0</sup> species is trapped by starting material to form the Pd<sup>I</sup>  $\mu$ -allyl dimer. Several experimental observations support this mechanism: (i) Propene was observed as a byproduct in the <sup>1</sup>H NMR spectrum when the reaction of **1** with K<sub>2</sub>CO<sub>3</sub> was monitored using <sup>1</sup>H NMR spectroscopy in *d*<sub>4</sub>-methanol, and propionaldehyde was detected by GC after the reaction of **1** with K<sub>2</sub>CO<sub>3</sub> in <sup>n</sup>PrOH. (ii) Reaction of **1** with K<sub>2</sub>CO<sub>3</sub> in *d*<sub>4</sub>-methanol was inhibited by the presence of excess <sup>n</sup>Bu<sub>4</sub>NCl in solution, as this presumably prevented initial coordination of *d*<sub>4</sub>-methanol. (iii) Facile activation of the monomeric precatalysts by K<sub>2</sub>CO<sub>3</sub> to form Pd<sup>I</sup>  $\mu$ -allyl dimers was observed only in primary alcohol solvents, such as MeOH, EtOH, <sup>n</sup>PrOH, and <sup>n</sup>BuOH, with a decrease in rate as the size of the alcohol increased, most likely due to steric factors. (iv) Only slow dimer formation was observed when **1** was heated at 40 °C in a *d*<sub>8</sub>-isopropanol suspension of K<sub>2</sub>CO<sub>3</sub>, as the increased steric bulk of <sup>1</sup>PrOH probably prevents it from readily displacing the chloride ligand and entering the proposed reaction pathway. (v) No reaction was observed when **1** and K<sub>2</sub>CO<sub>3</sub> were heated for 12 h at 60 °C in <sup>t</sup>BuOH, which is both sterically bulky and lacks the  $\beta$ -hydrogen necessary for activation. Overall, our synthetic protocol represents a novel and mild way to activate the (NHC)Pd( $\eta^3$ -allyl)Cl scaffold and suggests that the harsh base KO<sup>t</sup>Bu used by Nolan and others for catalysis is not necessary in the presence of primary alcohol solvents.<sup>9b,d</sup>

**Catalytic Studies.** The catalytic efficiency for the Suzuki–Miyaura reaction of the Pd<sup>II</sup> monomers and their Pd<sup>I</sup>  $\mu$ -allyl dimer congeners was compared using conditions similar to those reported by Nolan and co-workers from 25 to 40 °C (Table 1).<sup>9d</sup> A mixed solvent system<sup>32</sup> was utilized to ensure a homogeneous reaction mixture,<sup>33</sup> in contrast to the heterogeneous conditions used by Nolan. Unsubstituted complexes **1** and **4** are both poor precatalysts for this reaction, and dimer **4** outperforms **1** at all temperatures. The crotyl systems **2** and **5** are slightly more efficient precatalysts than the analogous unsubstituted allyl systems at all temperatures, but the same pattern holds, and dimer **5** always gives higher yields than **2**. A combination of factors could account for the improved catalytic activity of the dimers in the allyl and crotyl systems. As demonstrated in eq 1, **1** and **2** are not efficiently activated under our reaction conditions, whereas the dimeric systems are already partially activated and may generate the Pd<sup>0</sup> active species faster than the monomer. Moreover, the IPr–Pd<sup>0</sup> that is formed upon activation of **1** and **2** could be reacting with unreacted **1** and **2** to form the corresponding dimers **4** and **5** instead of entering the catalytic cycle. In contrast to the allyl and crotyl systems, the monomeric cinnamyl precatalyst **3** vastly outperforms its dimeric congener **6**. For example, a 95% yield was obtained after 60 min at 25 °C using precatalyst **3**, whereas the yield was only 3% using the corresponding dimer **6**. This disparity is inconsistent with complete conversion of **3**

Scheme 3. Proposed Mechanism for Formation of the  $\mu$ -Allyl Dimers 4–6 from Monomers 1–3 with Weak BaseTable 1. Yields<sup>a</sup> of Product for the Suzuki–Miyaura Reaction<sup>b</sup> Catalyzed by Complexes of the Type (IPr)Pd( $\eta^3$ -allyl)Cl (1–3) and Related Pd<sup>I</sup>  $\mu$ -Allyl Dimers (4–6)

temp (°C)	time (min)	% yields for precatalysts					
		1	4	2	5	3	6
25	30	<1	2	3	5	93	1
	60	2	7	14	22	95	3
30	30	4	4	19	30	>99	4
	60	13	17	36	69	>99	26
35	30	8	15	35	51	>99	20
	60	28	52	67	97	>99	97
40	30	20	32	58	92	>99	74
	60	81	93	80	99	>99	99

<sup>a</sup>Yields were calculated using gas chromatography with naphthalene as an internal standard and are the average of two runs. <sup>b</sup>Reaction conditions: <sup>i</sup>PrOH solution containing 0.625 M 4-chlorotoluene, 0.3125 M naphthalene, and 0.6875 M KO<sup>t</sup>Bu (800  $\mu$ L); MeOH solution containing 3.5 M phenylboronic acid (150  $\mu$ L); THF solution containing 0.1 M [Pd]<sub>tot</sub> (50  $\mu$ L).

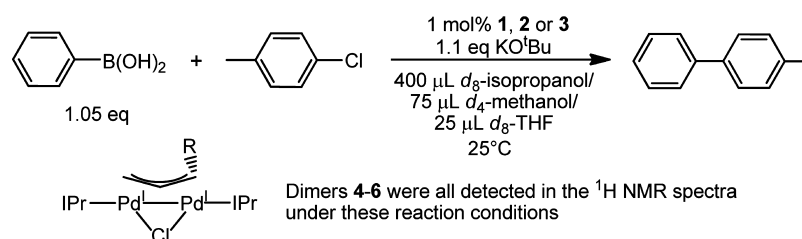
to **6** under the reaction conditions. The full set of monomeric and dimeric precatalysts was also screened for the Suzuki–Miyaura of more sterically hindered substrates (Table S1, Supporting Information), and similar catalytic results were obtained.<sup>24</sup> An interesting feature of the catalytic studies is the poor performance of precatalyst **2**. Under Nolan's heterogeneous reaction conditions **2** and **3** both had high activity,<sup>9d</sup> whereas under our conditions **3** gives significantly higher activity than **2**. Our control experiments indicate that under Nolan's conditions both **2** and **3** activate rapidly (see eq S1,

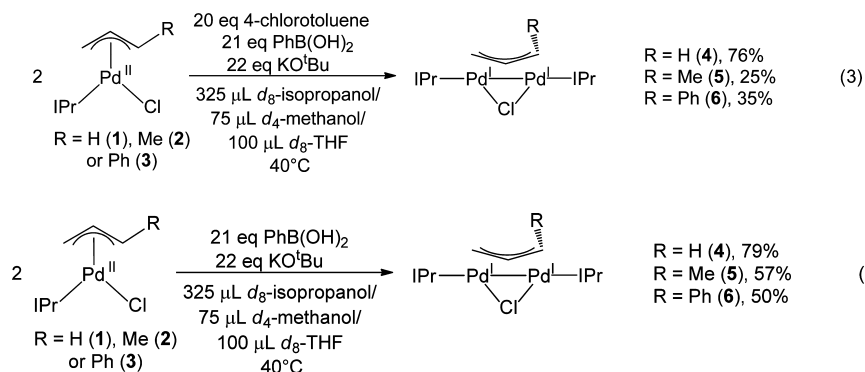
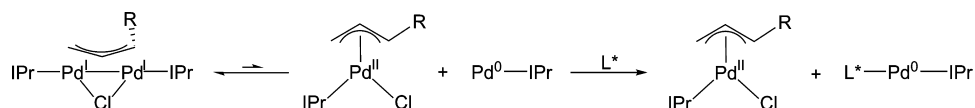
Supporting Information), whereas under our conditions only **3** activates quickly (eq 1).<sup>24</sup>

Direct evidence for the presence of Pd<sup>I</sup>  $\mu$ -allyl dimers under the catalytic conditions was obtained using NMR spectroscopy. When catalytic reactions with **1**, **2**, and **3** were tracked by <sup>1</sup>H NMR spectroscopy under conditions virtually identical to those described in Table 1 at room temperature (Scheme 4), signals corresponding to **4**, **5**, and **6**, respectively, were detected in the baseline of the <sup>1</sup>H NMR spectra. In all three systems resonances associated with the Pd<sup>I</sup>  $\mu$ -allyl dimers could be observed while the catalytic reactions were proceeding,<sup>24</sup> which indicates that Pd<sup>I</sup>  $\mu$ -allyl dimer formation is a process that can remove some of the active IPr–Pd<sup>0</sup> species during catalysis. The distinct <sup>1</sup>H NMR signals of the  $\mu$ -allyl ligands (*vide supra*) permitted unambiguous assignment of the dimers, but the trace concentration of these complexes compared to the catalytic substrates prevented accurate quantification of Pd<sup>I</sup>  $\mu$ -allyl dimer formation.<sup>24</sup>

Using modified catalytic conditions (eq 3) it was possible to quantify the formation of Pd<sup>I</sup>  $\mu$ -allyl dimers by <sup>1</sup>H NMR spectroscopy in reactions using **1**, **2**, and **3** as the precatalyst.<sup>24</sup> In the cases of the unsubstituted precatalyst **1** and the crotyl precatalyst **2**, a gradual increase in the dimer concentrations occurred as the catalytic reactions proceeded. When catalysis was complete, approximately 76% of the Pd was in the form of dimer **4** for precatalyst **1**, whereas for precatalyst **2**, only 25% of the Pd was in the form of **5**. For precatalyst **3**, approximately 35% of the Pd was in the form of **6** straight after mixing, and this percentage stayed relatively constant as the catalytic reaction proceeded. It is proposed that this increased rate of formation of **6** compared to **4** and **5** is due to the fast rate of activation of **3**.

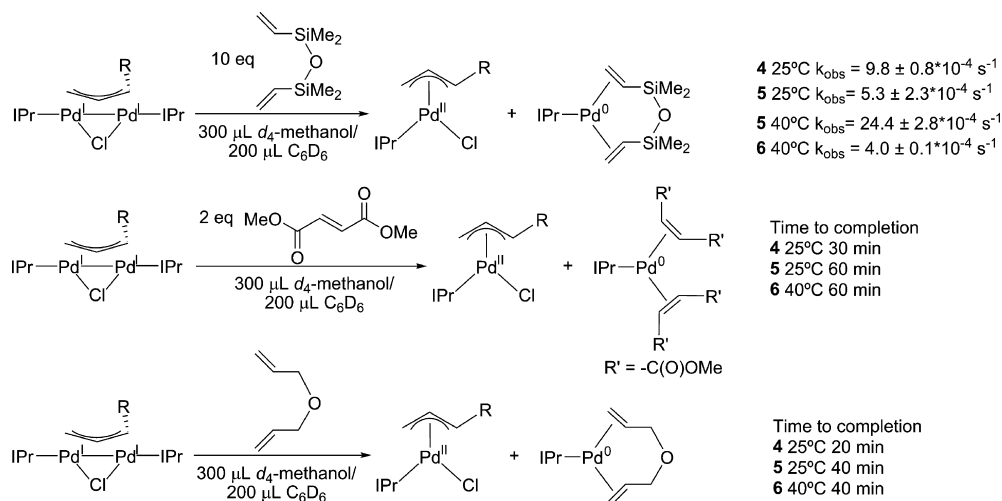
On the basis of the significant concentration of **4** observed under these modified conditions, we propose that the low

Scheme 4. Conditions Used for Detection of Dimers 4–6 by <sup>1</sup>H NMR Spectroscopy in Catalytic Reactions Using 1–3

Scheme 5. Proposed Disproportionation of  $\mu$ -Allyl Dimers<sup>a</sup>

<sup>a</sup>Addition of a trapping ligand L\* shifts the equilibrium to favor formation of two monomers.

Scheme 6. Summary of Disproportionation Experiments with 4–6 Using (a) dvds, (b) Dimethyl Fumarate, and (c) Allyl Ether as the Trapping Reagents



activity observed with precatalyst **1** is due not only to slow activation but also to the formation of significant quantities of the Pd<sup>I</sup>  $\mu$ -allyl dimer **4**. In contrast, only a fraction of the Pd in the substituted systems undergoes Pd<sup>I</sup>  $\mu$ -allyl dimer formation. One explanation for the low yields of the 1-substituted dimers is that formation of **5** and **6** from **2** and **3**, respectively, is less facile than formation of **4** from **1**. In this scenario, more of the IPr–Pd<sup>0</sup> formed from the activation can enter the catalytic cycle instead of reacting with **2** or **3** to form the corresponding dimers (Scheme 2). This hypothesis was tested by quantifying the formation of the Pd<sup>I</sup>  $\mu$ -allyl dimers under identical reaction conditions to eq 3 in the absence of the 4-chlorotoluene substrate (eq 4). Consistent with the scenario proposed in Scheme 2, the yield of the unsubstituted dimer **4** was unaffected by the presence of 4-chlorotoluene in solution, whereas the yields of the substituted dimers **5** and **6** were lower in the presence of 4-chlorotoluene. The proposed reaction pathway outlined in Scheme 2 is also consistent with the observation that precatalyst **2** outperforms **1** in catalysis (Table 1), even though the two precatalysts are activated at a comparable rate under our reaction conditions (eq 1). In the case of **2** more

IPr–Pd<sup>0</sup> can enter the catalytic cycle. The specific reasons for the differences in yields of the dimers from precatalysts **1**–**3** were investigated in detail and are discussed below.

**NMR Studies of the Activation of Pd<sup>I</sup>  $\mu$ -Allyl Dimers via Disproportionation.** Although several studies report the use of Pd<sup>I</sup>  $\mu$ -allyl dimers as precatalysts for cross-coupling, the mechanism of activation of these species is unclear.<sup>19,22</sup> Our catalytic results with **4**, **5**, and **6** indicate that the substitution on the  $\mu$ -allyl ligand has a profound effect on the activity. Furthermore, the similar catalytic performance of the dimers at elevated temperature suggests that in all three cases the same active catalyst is formed and that the disparity in activity at lower temperatures could simply be related to differences in the rates of activation. Therefore, we were interested in probing the mechanism of activation of Pd<sup>I</sup>  $\mu$ -allyl dimer precatalysts. Previously, while studying the insertion of CO<sub>2</sub> into Pd<sup>I</sup> dimers with two  $\mu$ -allyl ligands we suggested that these dimers can disproportionate into a monoligated Pd<sup>0</sup> species and a Pd<sup>II</sup> species, and others have proposed similar reactions.<sup>20e,25a,27,34</sup> In this case, we propose that **4**–**6** are activated through an analogous disproportionation, in which Pd(IPr)( $\eta^3$ -allyl)Cl

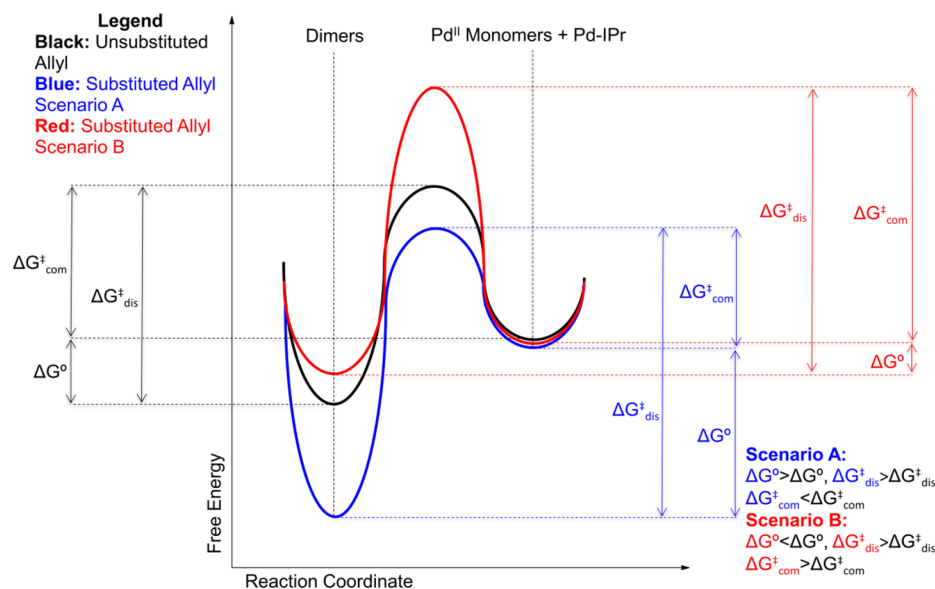


**Figure 6.** Reaction coordinate diagram illustrating two different scenarios for the relative rates of comproportionation of 1-substituted species compared to unsubstituted species, based on the relative rates of disproportionation summarized in Scheme 6. In Scenario A, 1-substituted Pd<sup>I</sup>  $\mu$ -allyl dimers are thermodynamically stabilized and no information from the relative rates of disproportionation can be obtained about the relative rates of comproportionation (we have arbitrarily shown the barrier as smaller). In Scenario B, 1-substituted Pd<sup>I</sup>  $\mu$ -allyl dimers are not thermodynamically stabilized and the relative rates of comproportionation will be directly related to the rates of disproportionation.

(1–3) and catalytically active IPr–Pd<sup>0</sup> are formed (Scheme 5). The disproportionation is thermodynamically unfavorable but can be driven by trapping the IPr–Pd<sup>0</sup> product. We hypothesized that the rate of disproportionation will be related to the catalytic performance of  $\mu$ -allyl dimer precatalysts.

The rates of disproportionation of 4–6 in the presence of 10 equiv of 1,3-divinyl-1,1,3,3-tetramethyldisiloxane (dvds) (Scheme 6a), 2 equiv of dimethyl fumarate (Scheme 6b), and 1 equiv of allyl ether (Scheme 6c) were measured. The disappearance of dimer over time was tracked using <sup>1</sup>H NMR spectroscopy, and the rate of trapping is 4 > 5 ≫ 6 for all three trapping reagents. We conclude from these experiments that increasing the steric bulk at the 1-position of the  $\mu$ -allyl ligand increases the kinetic barrier to disproportionation. At first glance these results appear inconsistent with our catalytic results, which indicated that under all conditions the crotyl dimer 5 was more active than the unsubstituted dimer 4 and that under some conditions the cinnamyl dimer 6 is more active than 4. However, we believe that the overall efficiency of a Pd<sup>I</sup> dimer for catalysis is determined by both the rate of disproportionation and the rate at which the subsequent (IPr)Pd( $\eta^3$ -allyl)Cl product is activated and can enter the catalytic cycle. For example, although disproportionation of the crotyl dimer 5 is slower than the unsubstituted dimer 4, the crotyl monomer 2 is a better precatalyst than 1, so overall 5 outperforms 4. A similar argument explains why 6, which undergoes slow disproportionation, is a better precatalyst than 4 under some reaction conditions.

Our experiments clearly indicate that the rate of disproportionation is dependent on the trapping reagent. Allyl ether is the fastest trapping reagent, while the more sterically hindered dvds is the slowest. In fact, in the case of dvds, addition of 10 equiv was required to ensure that the reaction proceeded at a reasonable rate. Under these pseudo-first-order conditions we were able to demonstrate that there is a first-order dependence on both the Pd dimer and dvds.<sup>24</sup> Unfortunately from these experiments it is not possible to

determine the exact role that the trapping reagent plays in the reaction, and this is explored further computationally (*vide infra*). Interestingly, the rate of disproportionation is also dependent on the solvent. Trapping experiments were performed in the presence of *d*<sub>4</sub>-methanol (with some C<sub>6</sub>D<sub>6</sub> present to solubilize the reaction mixtures) because coordinating solvents enhance the rate of disproportionation. For example, reaction of 5 with 10 equiv of dvds proceeded faster in the presence of the more strongly coordinating *d*<sub>3</sub>-ACN instead of *d*<sub>4</sub>-methanol. Specifically, the reaction was complete after 30 min in a 3:2 *d*<sub>3</sub>-ACN:C<sub>6</sub>D<sub>6</sub> mixture, whereas the reaction was complete after 90 min in 3:2 *d*<sub>4</sub>-methanol:C<sub>6</sub>D<sub>6</sub>.

**Studies on Comproportionation to form Pd<sup>I</sup>  $\mu$ -Allyl Dimers.** In catalysis using dimers as the precatalyst it is proposed that the rate of disproportionation to form the active IPr–Pd<sup>0</sup> species is important for high activity. However, in systems where a monomeric precatalyst is utilized, dimer formation from comproportionation of IPr–Pd<sup>0</sup> and the starting precatalyst (the microscopic reverse of disproportionation of the dimer) will lead to reduced rates by sequestering active catalyst. Therefore, we were interested in probing the kinetics of comproportionation from 1–3 and monoligated Pd<sup>0</sup>. Although the experiments in Scheme 6 show that increasing the sterics at the 1-position of the  $\mu$ -allyl ligand raises the kinetic barrier to disproportionation compared to the unsubstituted species, we cannot conclude from these experiments alone that this same relationship holds for comproportionation. As shown in Figure 6, the kinetic barrier to disproportionation could arise from thermodynamic stabilization of the 1-substituted Pd<sup>I</sup>  $\mu$ -allyl dimers (Figure 6, Scenario A), in which case the kinetic barrier to comproportionation could be smaller, the same, or larger than that observed for an unsubstituted species, and our disproportionation experiments do not provide us with any information about comproportionation. (In Figure 6, Scenario A, we have arbitrarily drawn the barrier as smaller.) On the other hand, if the substituted dimers are thermodynamically destabilized relative to the unsubstituted

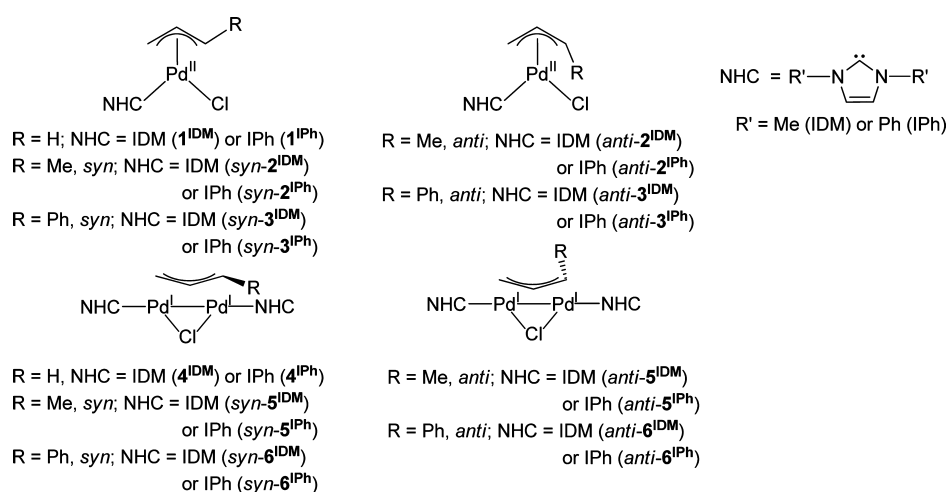
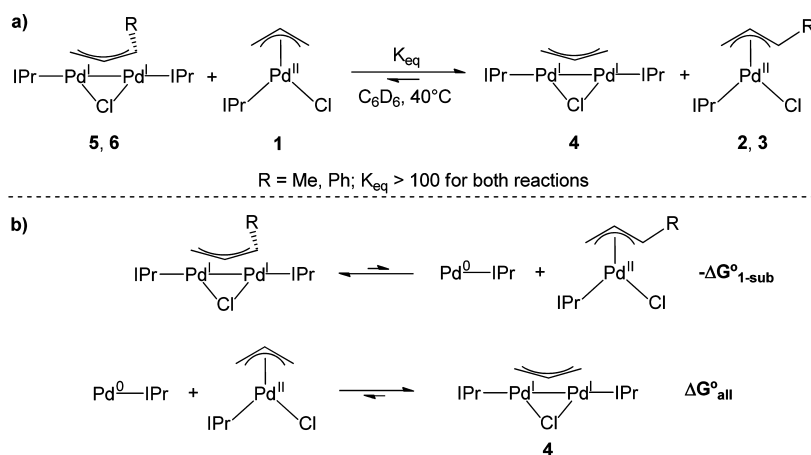
Scheme 7. Summary of Cross-Over Experiments Between the Pd<sup>I</sup>  $\mu$ -Allyl Dimers 5 and 6 and the Pd<sup>II</sup> Monomer 1

Figure 7. Structures of model compounds used in our calculations.

dimer then the higher kinetic barrier to disproportionation in 1-substituted species must arise from an increase in the relative transition state energies (Figure 6, Scenario B). In this case the relative kinetic barrier for the microscopic reverse comproportionation process will also be higher in 1-substituted systems.

To determine if Scenario A or Scenario B is operative, cross-over experiments were run in which the unsubstituted monomer **1** was mixed with the substituted dimers **5** and **6** (Scheme 7a).<sup>35</sup> The cross-over reactions can be described as the combination of the disproportionation of the substituted dimers and the comproportionation of **1** with IPr-Pd<sup>0</sup> (Scheme 7b). The equilibrium strongly favors formation of the unsubstituted allyl dimer **4** from the substituted allyl dimers **5** and **6**. This indicates that the comproportionation reaction to form **4** is more exergonic than the comproportionation reactions to form **5** or **6** ( $|\Delta G^{\circ}_{all}| > |\Delta G^{\circ}_{1-sub}|$  in Scheme 7b). Given that **5** and **6** are less thermodynamically stabilized than **4**, the slower rates of disproportionation for **5** and **6** must arise from an increase in the transition state energy for disproportionation/comproportionation (Scenario B in Figure 6).

The experiments in Schemes 6 and 7 provide a rationale for the disparity in the catalytic performance between monomeric precatalyst **3** and its dimeric congener **6** (Table 1). The increased steric bulk of the phenyl group on the 1-position of

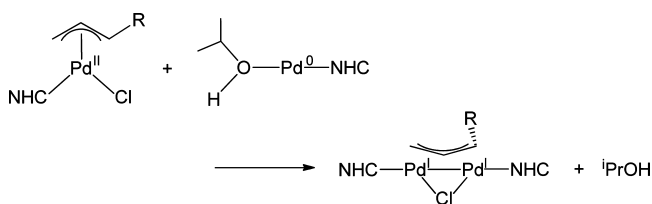
the cinnamyl ligand increases the transition state energy for disproportionation and comproportionation. Precatalyst **6** is inefficient because its kinetic barrier to disproportionation prevents it from readily accessing the catalytically active IPr-Pd<sup>0</sup>. Precatalyst **3** is highly effective not only because it is rapidly activated to the catalytically active IPr-Pd<sup>0</sup> but also because a relatively large kinetic barrier to comproportionation slows down formation of the less active **6** from unreacted **3** and IPr-Pd<sup>0</sup>, a deleterious process that removes the active catalyst from the reaction mixture. In this precatalyst system oxidative addition with the aryl halide substrate is more likely to outcompete comproportionation of IPr-Pd<sup>0</sup> with unreacted **3** compared to unsubstituted **1**, thus increasing the concentration of IPr-Pd<sup>0</sup> that enters the catalytic cycle (Scheme 2). However, direct observation of dimer **6** in catalytic reactions with **3** indicates that comproportionation still occurs in this system. In principle, even more active precatalysts could be designed by further increasing the barrier to dimerization. Alternatively, if the speed of activation is increased further by modifying the precatalyst, it may be possible to develop highly active systems in which all of the Pd<sup>II</sup> precatalyst is converted to Pd<sup>0</sup>, before deleterious comproportionation between Pd<sup>II</sup> and Pd<sup>0</sup> can occur.

**Computational Studies on Comproportionation and Disproportionation.** DFT calculations were performed to further evaluate the effect of substituents on the 1-position of

the allyl ligand on the kinetics and thermodynamics of the disproportionation/comproportionation pathway. Calculations were performed with two different simplified NHC ligands, IDM and IPh, where the steric bulk of the IPr ligand was reduced to different degrees (Figure 7).<sup>36</sup> In the case of the 1-substituted monomers and dimers, isomers with both *syn* and *anti* conformations of the  $\eta^3$ -allyl or  $\mu$ -allyl ligand were modeled. In general, the relative energies of the isomers are in agreement with our experimental results, and isomers with *syn* conformations of the 1-substituted  $\eta^3$ -allyl ligand are the most stable for monomeric compounds, while isomers with *anti* conformations of the  $\mu$ -allyl ligand are the most stable for the dimeric compounds.<sup>24</sup> This suggests that our computational method is suitable for modeling the relative stabilities of these complexes. Furthermore, where calculated structures could be directly compared with experimental structures, close agreement between the theoretical and the experimental bond distances and angles was observed.<sup>24</sup>

The thermodynamics of  $\mu$ -allyl dimer formation through comproportionation of Pd<sup>II</sup> complexes of the type Pd(L)( $\eta^3$ -allyl)Cl and L–Pd<sup>0</sup> were calculated (Table 2). The monoligated Pd<sup>0</sup> complexes were modeled with an explicit solvent molecule coordinated to Pd to complete the coordination sphere. <sup>i</sup>PrOH was selected as the solvent, because this was the primary solvent used in catalytic reactions (*vide supra*). The calculations indicate that dimer formation is strongly preferred in all cases, in agreement with the exergonic character of the comproportionation reactions observed experimentally. For systems supported by the IDM ligand, formation of *anti*-5<sup>IDM</sup> is the most thermodynamically favorable, although there is only a small difference in the calculated energy of dimer formation for the unsubstituted, crotyl and cinnamyl species. Calculations with IPh reveal a different trend. In this case formation of the unsubstituted species 4<sup>IPh</sup> is the most thermodynamically favored. The small yet significant energy differences between the three systems with the IPh ligand show the influence of steric bulk in the 1-position of the  $\mu$ -allyl ligand on the relative stability of the Pd<sup>I</sup> dimers.

**Table 2. Calculated Thermodynamics for Formation of Pd<sup>I</sup>  $\mu$ -Allyl Dimers through Comproportionation of Monomers of the Type Pd(NHC)( $\eta^3$ -allyl)Cl and Monoligated Pd<sup>0</sup>**

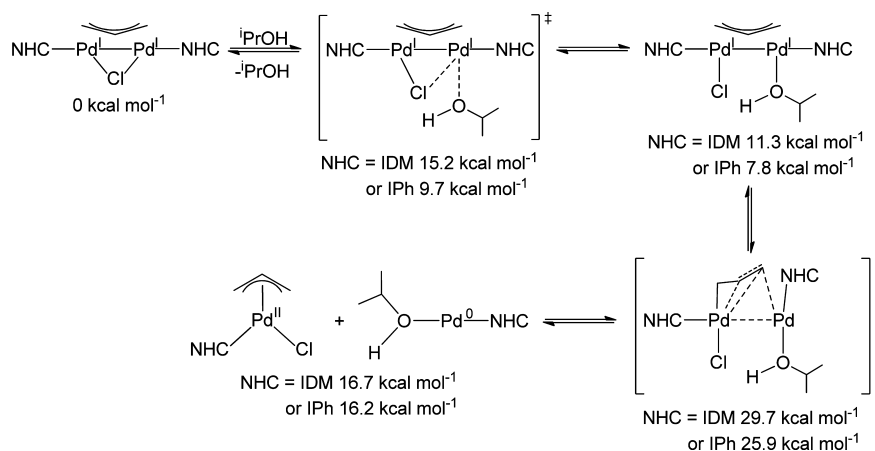


	$\Delta G_{\text{com}}^{\circ}$ (kcal mol <sup>-1</sup> )
4 <sup>IDM</sup>	-16.7
<i>anti</i> -5 <sup>IDM</sup>	-17.3 <sup>a</sup>
<i>anti</i> -6 <sup>IDM</sup>	-15.0 <sup>a</sup>
4 <sup>IPh</sup>	-16.2
<i>anti</i> -5 <sup>IPh</sup>	-13.4 <sup>a</sup>
<i>anti</i> -6 <sup>IPh</sup>	-15.5 <sup>a</sup>

<sup>a</sup>Calculated numbers are for comproportionation from the *syn* isomers of the 1-substituted monomers to the *anti* isomers of the  $\mu$ -allyl dimers, as these are the thermodynamically preferred isomers.

Experimentally, when the unsubstituted monomer 1 was mixed with the 1-substituted dimers 5 or 6, we observed essentially complete conversion to the unsubstituted dimer 4 and the 1-substituted monomers 2 or 3 (Scheme 7). Within error, the calculated equilibrium constants for cross-over reactions between the monomer 1<sup>IPh</sup> and the dimers *anti*-5<sup>IPh</sup> and *anti*-6<sup>IPh</sup> are consistent with these results. The calculated  $K_{\text{eq}}$  at 25 °C for cross over between 1<sup>IPh</sup> and *anti*-5<sup>IPh</sup> is 130, while for 1<sup>IPh</sup> and *anti*-6<sup>IPh</sup> the value is 3. When the full IPr ligand was used,<sup>24</sup> the calculations give even better agreement with the experimental results. At 25 °C, the calculated  $K_{\text{eq}}$  value for cross over between 1 and 5 is 83, while for 1 and 6 the value is 1091. Therefore, we conclude that in an analogous fashion to experimental results calculations with the more sterically bulky IPh and IPr ligands suggest that formation of 1-substituted dimers through comproportionation is less thermodynamically favorable than formation of the unsubstituted dimer.

Three main pathways were computationally tested to provide information about the activation of  $\mu$ -allyl dimers: (i) disproportionation to generate a solvent (<sup>i</sup>PrOH) stabilized monoligated Pd<sup>0</sup> species and a complex of the type Pd(NHC)( $\eta^3$ -allyl)Cl, (ii) homolytic scission of the Pd–Pd bond to generate two Pd<sup>I</sup> monomers, and (iii) disproportionation to generate an anionic Pd<sup>0</sup> monomer and a cationic Pd<sup>II</sup> monomer. Pathways (ii) and (iii) are significantly higher in energy than pathway (i) and are discussed further in the Supporting Information.<sup>24</sup> Pathway (i) is a two-step process, which requires solvent assistance (Scheme 8). In the first step, the bridging chloride ligand on one Pd atom is displaced by <sup>i</sup>PrOH to form an intermediate with a  $\mu$ -allyl ligand and terminal Pd–Cl and Pd–<sup>i</sup>PrOH groups. The coordination of <sup>i</sup>PrOH is slightly energetically uphill and goes through a relatively low-energy transition state in which one of the Pd–Cl bonds is almost completely cleaved and a new bond between Pd and <sup>i</sup>PrOH is being formed. This transition state is similar to those observed for ligand substitution at monomeric centers which proceed via a dissociative interchange mechanism.<sup>29</sup> An alternative pathway in which <sup>i</sup>PrOH coordination results in conversion of the  $\mu$ -allyl ligand into an  $\eta^1$ -allyl ligand and the bridging chloride ligand remains intact is considerably higher in energy.<sup>24</sup> In the second step, a Pd–C bond of the  $\mu$ -allyl ligand and the Pd–Pd bond are cleaved to generate two monomeric fragments. The Pd atom to which <sup>i</sup>PrOH binds undergoes Pd–C bond cleavage. The transition state for Pd–C and Pd–Pd bond breakage is the highest energy point on the reaction pathway. The transition state for disproportionation of 4<sup>IPh</sup> (TS-4<sup>IPh</sup><sub>dis</sub>), which is virtually identical to the transition state for disproportionation of 4<sup>IDM</sup>, is shown in Figure 8. In this late transition state the dimer has almost been completely cleaved, and the Pd–Pd distance is 3.18 Å, compared to 2.65 Å in 4<sup>IPh</sup>. One of the Pd atoms is essentially two coordinate and in a linear geometry, with IPh and <sup>i</sup>PrOH supporting ligands. The closest Pd–C contact from a carbon atom of the initial  $\mu$ -allyl ligand to the two coordinate Pd atom is 2.74 Å, while the Pd–Cl distance is 3.53 Å. The other Pd atom is four coordinate and in a distorted square planar geometry, with IPh, and chloride ligands, along with the incipient  $\eta^3$ -allyl ligand. The incipient  $\eta^3$ -allyl ligand is bound through two C atoms with Pd–C bond lengths of 2.10 and 2.28 Å, respectively, while the other Pd–C distance is 2.72 Å. The Pd–Cl distance of 2.68 Å is slightly elongated compared with the calculated Pd–Cl distance in 1<sup>IPh</sup> (2.52 Å). Finally, it should be noted that a pathway in which isopropoxide assists in cleavage of the dimer instead of <sup>i</sup>PrOH

Scheme 8. Calculated Pathway and Free Energies for Solvent-Assisted Disproportionation of  $4^{\text{IDM}}$  or  $4^{\text{IPh}}$ <sup>a</sup>

<sup>a</sup>The energy of the dimer and <sup>i</sup>PrOH is defined as being at 0 kcal mol<sup>-1</sup>.

has the same kinetic barrier to disproportionation as the pathway involving <sup>i</sup>PrOH but is unlikely due to the relative concentrations of isopropoxide versus <sup>i</sup>PrOH under the catalytic reaction conditions.<sup>24</sup>

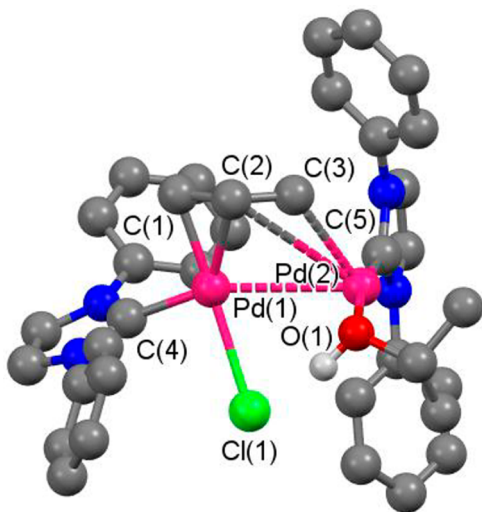


**Figure 8.** Calculated transition state for disproportionation of  $4^{\text{IPh}}$  (TS- $4^{\text{IPh}}_{\text{dis}}$ ) (selected hydrogen atoms have been omitted for clarity). Selected bond lengths (Angstroms) and angles (degrees): Pd(1)–Pd(2) 3.18, Pd(1)–C(1) 2.10, Pd(1)–C(2) 2.28, Pd(1)–C(3) 2.72, Pd(1)–C(4) 2.20, Pd(1)–Cl(1) 2.68, Pd(2)–C(5) 1.99, Pd(1)–O(1) 2.27, Pd(2)–C(3) 2.74, C(1)–C(2) 1.44, C(2)–C(3) 1.39, C(1)–Pd(1)–C(4) 94.4, C(1)–Pd(1)–Cl(1) 167.6, C(5)–Pd(2)–O(1) 169.1.

The energies of the transition states for disproportionation of 1-substituted and unsubstituted  $\mu$ -allyl dimers with both IDM and IPH supporting ligands are compared in Table 3. In the case of the 1-substituted dimers, calculations were performed starting from the *anti* isomers. The computed reaction pathway leads to formation of the thermodynamically disfavored *anti* isomer of the 1-substituted monomers of the type Pd(NHC)-( $\eta^3$ -allyl)Cl. However, these types of monomeric systems are known to undergo facile isomerization from *anti* to *syn*,<sup>37</sup> which is consistent with our observation that the *syn* isomers were exclusively the final product in our trapping experiments.<sup>38</sup> The transition state energies and structures for disproportionation

**Table 3.** Calculated Barriers for Solvent (<sup>i</sup>PrOH) Assisted Disproportionation and Comproportionation of Pd<sup>I</sup>  $\mu$ -Allyl Dimers with Monomers of the Type Pd(NHC)( $\eta^3$ -allyl)Cl and Monoligated Pd<sup>0</sup>

	$\Delta G_{\text{dis}}^{\ddagger}$ (kcal mol <sup>-1</sup> )	$\Delta G_{\text{com}}^{\ddagger}$ (kcal mol <sup>-1</sup> )
$4^{\text{IDM}}$	29.7	13.0
<i>anti</i> - $5^{\text{IDM}}$	29.3	12.0 <sup>a</sup>
<i>anti</i> - $6^{\text{IDM}}$	28.4	13.4 <sup>a</sup>
$4^{\text{IPh}}$	25.9	9.6
<i>anti</i> - $5^{\text{IPh}}$	32.6	19.2 <sup>a</sup>
<i>anti</i> - $6^{\text{IPh}}$	33.8	18.3 <sup>a</sup>
<i>syn</i> - $5^{\text{IDM}}$		10.2
<i>syn</i> - $6^{\text{IDM}}$		11.1
<i>syn</i> - $5^{\text{IPh}}$		16.8
<i>syn</i> - $6^{\text{IPh}}$		14.6

<sup>a</sup>Calculated numbers are the barrier for comproportionation starting from the *syn* isomer of the 1-substituted monomers. The pathway for this process presumably involves isomerization from the *syn* isomer of the monomer to the *anti* isomer.

of unsubstituted, crotyl and cinnamyl  $\mu$ -allyl dimers are virtually identical with the sterically undemanding IDM ligand, and the structures are similar to that described for TS- $4^{\text{IPh}}_{\text{dis}}$  (Figure 8). In contrast, when the sterically bulky IPH ligand is utilized, the transition state energies for the 1-substituted species are significantly higher than that for the unsubstituted species. This is qualitatively in agreement with our experimental results that disproportionation is faster for the unsubstituted species, and our comparative calculations with the IDM and IPH ligands indicate that the origin of this effect is related to steric rather than electronic factors. A comparison of the calculated structure of the transition state for disproportionation of *anti*- $6^{\text{IPh}}$  (TS- $6^{\text{IPh}}_{\text{dis}}$  Figure 9) with TS- $4^{\text{IPh}}_{\text{dis}}$  reveals major differences. For example, in TS- $6^{\text{IPh}}_{\text{dis}}$  the two Pd-containing fragments are even more separated. The Pd–Pd distance is 3.59 Å, and the closest Pd–C contact from a carbon atom of the initial  $\mu$ -cinnamyl ligand to the two-coordinate Pd atom is 3.00 Å. Furthermore, although the incipient  $\eta^3$ -cinnamyl ligand on the square planar Pd is still bound through two C atoms, the Pd–C distances are longer (2.10, 2.41, and 3.07 Å). Apart from the increased

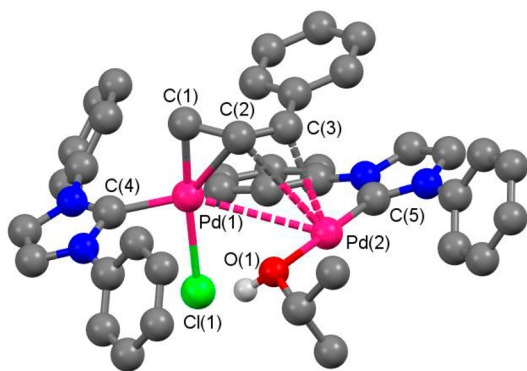


**Figure 9.** Calculated transition state for disproportionation of *anti-6*<sup>IPh</sup> (TS-6<sup>IPh</sup><sub>dis</sub>) (selected hydrogen atoms have been omitted for clarity). Selected bond lengths (Angstroms) and angles (degrees): Pd(1)–Pd(2) 3.59, Pd(1)–C(1) 2.10, Pd(1)–C(2) 2.41, Pd(1)–C(3) 3.07, Pd(1)–C(4) 2.00, Pd(1)–Cl(1) 2.67, Pd(2)–C(5) 1.99, Pd(1)–O(1) 2.23, Pd(2)–C(3) 3.00, C(1)–C(2) 1.44, C(2)–C(3) 1.39, C(1)–Pd(1)–C(4) 98.7, C(1)–Pd(1)–Cl(1) 174.4, C(5)–Pd(2)–O(1) 180.0.

separation of the two fragments, the other major difference between TS-4<sup>IPh</sup><sub>dis</sub> and TS-6<sup>IPh</sup><sub>dis</sub> is the orientation of the IPh ligand around the two-coordinate Pd center. In TS-4<sup>IPh</sup><sub>dis</sub> the five-membered imidazol-2-ylidene ring of this IPh ligand is perpendicular to the plane containing the two Pd atoms and the carbon donor of the IPh ligand. In contrast, in TS-6<sup>IPh</sup><sub>dis</sub> the imidazol-2-ylidene ring is almost parallel to this plane, presumably for steric reasons. The transition state structure for disproportionation of *anti-5*<sup>IPh</sup> is more similar to TS-6<sup>IPh</sup><sub>dis</sub> than to TS-4<sup>IPh</sup><sub>dis</sub>, consistent with the increased barrier.

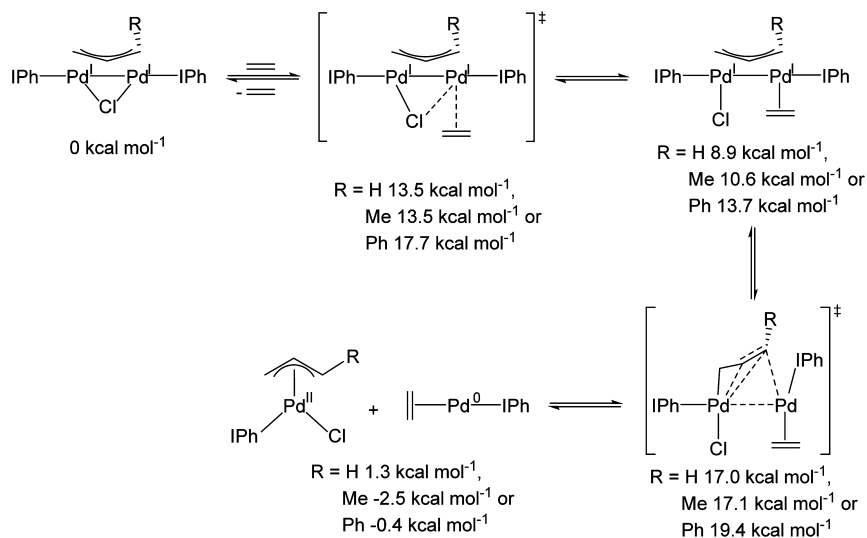
In our experiments exploring the disproportionation of dimers 4–6 we noticed a pronounced effect of both the trapping agent and the solvent on the rate of the reaction. As a simple model for our olefin-based trapping reagents disproportionation of the dimers 4<sup>IPh</sup>, *anti-5*<sup>IPh</sup>, and *anti-6*<sup>IPh</sup> were modeled in the presence of ethylene (Scheme 9). The calculated pathway for disproportionation is virtually identical to that described for the <sup>1</sup>PrOH-mediated process, with

ethylene initially binding to one Pd atom along with cleavage of a Pd–Cl bond. However, the critical energy barrier associated with cleavage of the Pd–Pd and Pd–C bonds is lowered for all three systems when compared to that found for <sup>1</sup>PrOH. This may be due to back-donation from the metal to ethylene, which should stabilize the incipient Pd<sup>0</sup> oxidation state in the transition state. Our computational results clearly indicate that the nature of the coordinating solvent or trapping agent can directly affect the rate of disproportionation, consistent with our experimental results. Also in agreement with our experimental results, the calculated barriers for disproportionation with ethylene follow the order 4<sup>IPh</sup> ≈ *anti-5*<sup>IPh</sup> ≪ *anti-6*<sup>IPh</sup>. Thus, the calculations predict that increasing the sterics at the 1-position of the μ-allyl ligand results in an increased calculated barrier to disproportionation in both the ethylene- and the <sup>1</sup>PrOH-assisted pathways. However, in the <sup>1</sup>PrOH-assisted pathway, the barrier for disproportionation of *anti-5*<sup>IPh</sup> is significantly closer in energy to that of *anti-6*<sup>IPh</sup> than 4<sup>IPh</sup>.

Overall, our calculations provide clear support for the hypothesis that the disproportionation of Pd<sup>I</sup> dimers into a monoligated Pd<sup>0</sup> complex and a Pd<sup>II</sup> complex of the type Pd(L)(η<sup>3</sup>-allyl)Cl is the pathway for generation of the Pd<sup>0</sup> active species in catalysis. Although this process is thermodynamically unfavorable, under catalytic conditions the aryl halide substrate can trap the Pd<sup>0</sup> species via oxidative addition, which provides a driving force for disproportionation. Given that the pathway for disproportionation is assisted by solvent coordination, we suggest that for faster activation in coupling reactions with μ-allyl dimer precatalysts a weakly coordinating solvent such as <sup>1</sup>PrOH or ACN should be present and that these reactions should not be performed in pure hydrocarbon solvents, which are the conditions most commonly utilized in the literature.<sup>19,22c,d</sup>

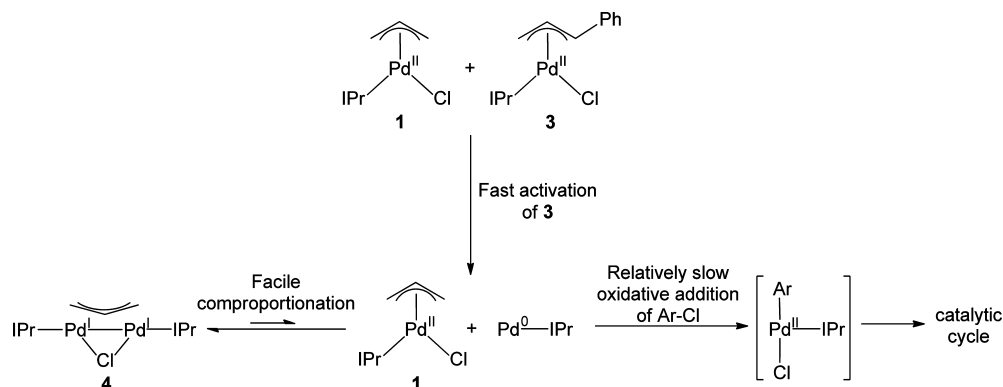
The calculated trends for the activation energies of comproportionation in the presence of <sup>1</sup>PrOH are the same as for disproportionation (Table 3). Formation of compounds with 1-substituted μ-allyl ligands species have significantly larger barriers than unsubstituted species when steric factors are considered. In the case of 1-substituted species, the kinetic

### Scheme 9. Calculated Pathway and Free Energies for Ethylene-Assisted Disproportionation of 4<sup>IPh</sup>, *anti-5*<sup>IPh</sup>, and *anti-6*<sup>IPh</sup><sup>a</sup>



<sup>a</sup>The energy of the dimer and ethylene is defined as being at 0 kcal mol<sup>-1</sup>.

Scheme 10. Inhibition of the Catalytic Activity of 3 by 1



products of comproportionation are predicted to be the *syn* isomers of the dimers, formed from the thermodynamically more stable *syn* isomers of monomers of the type Pd(NHC)-( $\eta^3$ -allyl)Cl. This is consistent with our experimental results, where during the synthesis of **5** initially a mixture of *syn* and *anti* isomers was formed, which equilibrated exclusively to the *anti* isomer over time. We believe that the pathway for formation of the thermodynamically preferred *anti*  $\mu$ -crotyl or  $\mu$ -cinnamyl dimers involves the initial facile isomerization of the starting  $\eta^3$ -allyl monomer to the *anti* conformation<sup>37</sup> followed by comproportionation of the *anti* monomer with L-Pd<sup>0</sup>. The computational results suggest that the crotyl monomer **2** is slightly less likely to undergo comproportionation with L-Pd<sup>0</sup> than the cinnamyl monomer **3**. This is in agreement with the experiments summarized in eq 3, where approximately equal yields of the substituted dimers **5** and **6** were observed under modified catalytic conditions using precatalysts **2** and **3**, respectively. On this basis we propose that the reason **2** is not a good precatalyst under our reaction conditions is due primarily to slow activation, not significant dimer formation. Further evidence in support of this hypothesis is provided by the results of Nolan and co-workers, who observed that **2** is a very efficient precatalyst under their heterogeneous reaction conditions,<sup>9d</sup> where we believe that activation of **2** is rapid.<sup>24</sup> Essentially, if precatalysts **2** and **3** are activated at the same rate both species will give similar catalytic results as they are both equally likely to form the off-cycle dimer. In contrast, even if **1** is activated at the same rate as **2** and **3**, it will give lower activity in catalysis because it is more likely to comproportionate and form **4**.

**Inhibition of Catalysis by Precatalyst 1.** On the basis of the experiments in Schemes 6 and 7 and our computational results, it is clear that the barrier to comproportionation to form **4** from **1** and IPr-Pd<sup>0</sup> is significantly lower than the barrier to comproportionation in the 1-substituted systems. Therefore, we postulated that **1** could inhibit the catalytic performance of **3** by trapping the IPr-Pd<sup>0</sup> produced from activation of **3** as dimeric **4** (Scheme 10).

When a stock solution containing 1 mol % **1** and 1 mol % **3** was used for catalysis, a marked decrease in reaction rate was observed compared to the corresponding reaction in which **1** was absent, despite the increase in the overall Pd loading (Table 4). To provide support for our hypothesis that this reduced efficiency was due to formation of **4**, we performed a Suzuki–Miyaura reaction under modified catalytic conditions (2.5 mol % **1**, 2.5 mol % **3**, 40 °C) and monitored the Pd speciation using <sup>1</sup>H NMR spectroscopy.<sup>24</sup> At the end of the

Table 4. Yields<sup>a</sup> of Product for Suzuki–Miyaura Reactions<sup>b</sup> Inhibited by the Presence of **1** in Solution

temp (°C)	time (min)	% yields for precatalyst mixtures	
		<b>1</b> + <b>3</b>	1 mol % <b>4</b>
25	30	11	3
	60	24	9
30	30	11	6
	60	79	28
35	30	74	21
	60	92	64
40	30	83	46
	60	94	92

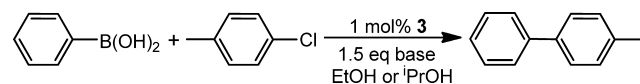
<sup>a</sup>Yields were calculated using gas chromatography with naphthalene as an internal standard and are the average of two runs. <sup>b</sup>Reaction conditions: <sup>i</sup>PrOH solution containing 0.625 M 4-chlorotoluene, 0.3125 M naphthalene, and 0.6875 M KO<sup>t</sup>Bu (800  $\mu$ L); MeOH solution containing 3.5 M phenylboronic acid (150  $\mu$ L); THF solution containing 0.1 M **1** and 0.1 M **3** or 0.1 M **4** (50  $\mu$ L).

reaction 68% of the Pd was in the form of **4**, with no significant amounts of **6** present. A control reaction was also performed to show that **4** is simply an off-cycle side product in this experiment that does not itself inhibit catalysis and that the perturbation in catalytic efficiency in Table 4 is due strictly to removal of active IPr-Pd<sup>0</sup> catalyst by comproportionation with **1**. When a stock solution containing 1 mol % **3** and 0.5 mol % **4** was used for catalysis, the reaction proceeded at the same rate as the corresponding reaction in the absence of **4**.<sup>24</sup> The results in Table 4 show that the extent of inhibition decreased with increasing temperature, presumably in part because at higher temperature **4** is more readily converted into monoligated IPr-Pd<sup>0</sup>. If all the IPr-Pd<sup>0</sup> formed from **3** had been trapped as **4** then the catalyst mixture of 1 mol % **1** and **3** would exhibit the same catalytic efficiency as 1 mol % **4**. The mixture of **1** and **3** outperforms a 1 mol % solution of **4**, suggesting that not all the IPr-Pd<sup>0</sup> is trapped as the Pd<sup>I</sup>  $\mu$ -allyl dimer. Nevertheless, the perturbation in the efficiency of precatalyst **3** in the presence of **1** demonstrates that a significant fraction of the active IPr-Pd<sup>0</sup> catalyst can be removed from the reaction mixture through Pd<sup>I</sup>  $\mu$ -allyl dimer formation.

**Catalysis under Milder Conditions.** As noted earlier, our new synthesis of Pd<sup>I</sup>  $\mu$ -allyl dimers using K<sub>2</sub>CO<sub>3</sub> under mild conditions suggests that the strong base KO<sup>t</sup>Bu is not necessary

for catalysis with precatalysts of the type  $(\text{IPr})\text{Pd}(\eta^3\text{-allyl})\text{Cl}$  (eq 2) provided a primary alcohol is present. Table 5

**Table 5. Yields<sup>a</sup> of Product for Suzuki–Miyaura Reactions<sup>b</sup> Using Precatalyst 3 and Weak Bases**



temp (°C)	time (min)	% yields for different base/solvent combinations			
		K <sub>2</sub> CO <sub>3</sub> EtOH	K <sub>3</sub> PO <sub>4</sub> EtOH	K <sub>2</sub> CO <sub>3</sub> <sup>i</sup> PrOH	K <sub>3</sub> PO <sub>4</sub> <sup>i</sup> PrOH
25	30	59	42	<1	<1
	60	88	75	<1	<1
40	30	88	56	3	2
	60	92	66	9	8

<sup>a</sup>Yields were calculated using gas chromatography with naphthalene as an internal standard and are the average of two runs. <sup>b</sup>Reaction conditions: EtOH or <sup>i</sup>PrOH solution containing 0.5263 M 4-chlorotoluene, 0.2632 M naphthalene, and 0.5526 M phenylboronic acid (950  $\mu\text{L}$ ); 0.75 mmol of K<sub>2</sub>CO<sub>3</sub> or K<sub>3</sub>PO<sub>4</sub>; THF solution containing 0.1 M 3 (50  $\mu\text{L}$ ).

summarizes our catalytic results using K<sub>2</sub>CO<sub>3</sub> and K<sub>3</sub>PO<sub>4</sub> as bases for the Suzuki–Miyaura reaction with precatalyst 3 in EtOH and <sup>i</sup>PrOH.<sup>39</sup> Use of EtOH instead of <sup>i</sup>PrOH greatly improves the efficiency of the reactions using weak bases, and efficient conversions are observed even at 25 °C. This is the first time a milder base has been shown to promote efficient Suzuki–Miyaura reactions at mild temperature using Nolan's cinnamyl precatalyst, and this result could expand the substrate scope of this catalytic system. Furthermore, it may be applicable to cinnamyl-supported systems which use other ancillary ligands.

## CONCLUSIONS

This work has established that the efficiency of the  $(\text{IPr})(\eta^3\text{-cinnamyl})\text{Cl}$  precatalyst and most likely other related 1-substituted species for the Suzuki–Miyaura reaction is not only due to facile activation of the precatalyst scaffold but also because this system exhibits an increased kinetic barrier to comproportionation to form the corresponding Pd<sup>I</sup>  $\mu$ -allyl dimer. However, Pd<sup>I</sup>  $\mu$ -allyl dimer formation, which is a deleterious process that removes the  $\text{IPr-Pd}^0$  active species from the reaction mixture, was still observed under catalytic conditions with this highly active precatalyst and shown to be a facile process in all the systems that were studied in this report. On the basis of these results, we propose that Pd<sup>I</sup>  $\mu$ -allyl dimer formation is a general phenomenon in reaction mixtures that use precatalysts of the type  $\text{Pd}(\text{L})(\eta^3\text{-allyl})\text{Cl}$ , which were previously thought to only involve Pd<sup>0</sup> and Pd<sup>II</sup> complexes. By increasing the barrier to comproportionation between Pd<sup>0</sup> and Pd<sup>II</sup> or by developing systems that activate sufficiently quickly so that all of the Pd<sup>II</sup> is converted to Pd<sup>0</sup> before comproportionation can occur it should be possible to develop precatalysts that are even more active.

This study has also elucidated new pathways for activation of precatalysts of the type  $\text{Pd}(\text{NHC})(\eta^3\text{-allyl})\text{Cl}$  as well as their dimeric Pd<sup>I</sup> congeners. Efficient activation of  $\text{Pd}(\text{IPr})(\eta^3\text{-allyl})\text{Cl}$  type precatalysts was observed under weakly basic reaction conditions in primary alcohol solvents, and reaction conditions for the Suzuki–Miyaura reaction were subsequently developed using the  $\text{Pd}(\text{IPr})(\eta^3\text{-cinnamyl})\text{Cl}$

precatalyst and mild bases. Solvent-assisted disproportionation of the dimers generate the monoligated  $\text{L-Pd}^0$  active catalyst as well as Pd<sup>II</sup> complexes of the type  $\text{Pd}(\text{IPr})(\eta^3\text{-allyl})\text{Cl}$ . This further demonstrates the close relationship between Pd<sup>II</sup> complexes with  $\eta^3\text{-allyl}$  ligands and Pd<sup>I</sup> dimers with  $\mu$ -allyl ligands and indicates that interconversion between the two species is significantly more facile than previously thought. Overall, we expect that this work will aid in the design of more efficient Pd precatalysts for cross-coupling that are supported by  $\eta^3\text{-allyl}$  or related ligands, and further studies toward this end are being conducted in our laboratory.

## EXPERIMENTAL SECTION

**General.** Experiments were performed under a dinitrogen atmosphere in an M-Braun drybox or using standard Schlenk techniques unless otherwise stated. Under standard glovebox conditions purging was not performed between uses of pentane, diethyl ether, benzene, toluene, and THF; thus, when any of these solvents were used, traces of all these solvents were in the atmosphere and could be found intermixed in the solvent bottles. Moisture- and air-sensitive liquids were transferred by stainless steel cannula on a Schlenk line or in a drybox. Pentane, THF, and toluene were dried by passage through a column of activated alumina followed by storage under dinitrogen. All commercial chemicals were used as received except where noted. MeOH (J. T. Baker), <sup>i</sup>PrOH (Macron Fine Chemicals), and 200 proof EtOH (Decon Laboratories Inc.) were not dried but degassed by sparging with dinitrogen for 1 h and stored under dinitrogen. Ethyl acetate (Fisher Scientific) and hexanes (Macron Fine Chemicals) were used as received. Potassium phosphate (97%), potassium *tert*-butoxide (99.99%, sublimed), naphthalene (99%), propionaldehyde (97%), dimethyl fumarate (97%), 4-chlorotoluene (98%), and 2-chloro-*m*-xylene (97%) were purchased from Aldrich. Potassium carbonate was purchased from Mallinckrodt. 1,3-Divinyltetramethyldisiloxane, allyl ether (98%), and 4-methylbiphenyl were purchased from TCI. Phenylboronic acid (98%), 2,6-dimethoxytoluene (98%), 1-naphthaleneboronic acid, <sup>n</sup>BuOH (99%), and <sup>i</sup>BuOH (99%) were purchased from Alfa Aesar. Phenylboronic acid was purified via flash chromatography using 2:1 ethyl acetate/hexanes.<sup>32,40</sup> Flash chromatography was performed on silica gel 60 (230–400 mesh, Fisher Scientific). Potassium phosphate and potassium carbonate were ground with a mortar and pestle and stored in an oven at 130 °C prior to use. 4-Chlorotoluene, 2-chloro-*m*-xylene, <sup>n</sup>PrOH, 1,3-divinyltetramethyldisiloxane, and <sup>n</sup>BuOH were degassed prior to use through three freeze–pump–thaw cycles. Deuterated solvents were obtained from Cambridge Isotope Laboratories. C<sub>6</sub>D<sub>6</sub> was dried over sodium metal and stored under nitrogen, while *d*<sub>4</sub>-methanol, *d*<sub>8</sub>-isopropanol, and *d*<sub>8</sub>-THF were not dried but degassed prior to use through three freeze–pump–thaw cycles. NMR spectra were recorded on Bruker AMX-400 and -500 and Varian-300 and -500 spectrometers at ambient probe temperatures unless noted. For variable-temperature NMR, the sample temperature was calibrated by measuring the distance between the OH and the CH<sub>2</sub> resonances in ethylene glycol (99%, Aldrich). Chemical shifts are reported with respect to residual internal protio solvent for <sup>1</sup>H and <sup>13</sup>C{<sup>1</sup>H} NMR spectra. Atom numbering for the peak assignments is given below. All assignments are based on two-dimensional <sup>1</sup>H, <sup>13</sup>C-HMQC, and HMBC experiments. Robertson Microlit Laboratories, Inc. performed the elemental analyses (inert atmosphere). Gas chromatography analyses (GC) were performed on a Shimadzu GC-2010 Plus apparatus equipped with a flame ionization detector and a Shimadzu SHRXL-SMS column (30 m, 250  $\mu\text{m}$  inner diameter, film 0.25  $\mu\text{m}$ ). The following conditions were utilized for GC analyses: flow rate 1.23 mL/min constant flow, column temperature 50 °C (held for 5 min), 20 °C/min increase to 300 °C (held for 5 min), total time 22.5 min. The response factor used to calculate GC yields was determined using a purchased sample of 4-methylbiphenyl (TCI). Literature procedures were used to prepare the following compounds: IPr, <sup>41</sup>  $\text{Pd}(\text{IPr})(\eta^3\text{-allyl})\text{Cl}$  (1),<sup>9a</sup>  $\text{Pd}(\text{IPr})(\eta^3\text{-crotyl})\text{Cl}$  (2),<sup>9d</sup> and

Pd(IPr)( $\eta^3$ -cinnamyl)Cl (**3**).<sup>9d</sup> Compounds **1**–**3** were stored on the benchtop, while IPr was stored in a glovebox under dinitrogen.

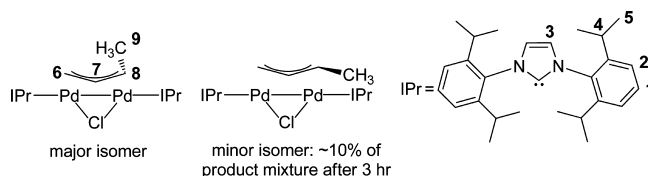
**X-ray Crystallography.** X-ray diffraction experiments were carried out on a Rigaku MicroMax-007HF diffractometer coupled to a Saturn994+ CCD detector with Cu K $\alpha$  radiation ( $\lambda = 1.54178$  Å) at  $-180$  °C. Crystals were mounted on MiTeGen polyimide loops with immersion oil. Data frames were processed using Rigaku CrystalClear and corrected for Lorentz and polarization effects. Using Olex2<sup>42</sup> the structure was solved with the XS<sup>43</sup> structure solution program by Patterson methods and refined with the XL<sup>43</sup> refinement package using least-squares minimization. Non-hydrogen atoms were refined anisotropically. Hydrogen atoms were refined using the riding model. Details of the crystal structure and refinement data for **5** and **6** are given in the Supporting Information.

**Computational Details.** DFT calculations were carried out using the Gaussian09 program.<sup>44</sup> Due to the rather large size of the systems studied, two different basis sets, BS1 and BS2, were used. With BS1, all elements were described with the full-electron double- $\zeta$  quality 6-31G basis set,<sup>45</sup> except the heaviest, Cl and Pd, which were described with the small-core SDD pseudopotential basis set.<sup>46</sup> BS1 was used in the geometry optimization and frequency calculations at the DFT-(M06L)<sup>47</sup>/SMD<sup>48</sup> level. The SMD continuum model was used to model the effects of the solvent (<sup>i</sup>PrOH;  $\epsilon = 19.264$ ). Geometries were fully optimized in solution without any geometry or symmetry constraints. Frequencies were computed analytically with the aim of identifying each stationary point as either a minimum (reactants, intermediates, and products) or a saddle point (transition states, TS). Transition state geometries were relaxed to reactants and products using the vibrational frequency data. Frequency calculations were also used to determine the difference between the potential ( $E$ ) and Gibbs ( $G$ ) energies,  $G - E$ , which contains the zero-point, thermal, and entropy energies. Potential energies were refined,  $E_{\text{sol}}$ , by means of single point (SP) calculations at the DFT(M06)/SMD level with a larger basis set, BS2. With BS2, all elements were described with a triple- $\zeta$  + polarization quality basis set, including the SDD(f,d) for Cl and Pd and the 6-311+G\*\* for all other elements.<sup>49</sup> The  $\Delta G$  and  $\Delta G^\ddagger$  values given in the text were obtained from the Gibbs energy in solution,  $G_{\text{sol}}$ , which was calculated by adding the thermochemistry corrections,  $G - E$ , to the refined SP energies,  $E_{\text{sol}}$ , i.e.,  $G_{\text{sol}} = E_{\text{sol}} + G - E$ .

**Synthetic Procedures and Characterizing Data for New Compounds.** ( $\mu$ -Allyl)( $\mu$ -Cl)Pd<sub>2</sub>(IPr)<sub>2</sub> (**4**). Pd(IPr)( $\eta^3$ -allyl)Cl (**1**) (101.7 mg, 0.178 mmol) and potassium carbonate (37 mg, 1.5 equiv) were transferred to a Schlenk flask and placed under dinitrogen. Degassed ethanol (5 mL) was transferred by cannula into the Schlenk flask at rt, and the reaction mixture was stirred at 40 °C for 3 h. Volatiles were removed under vacuum. The residue was extracted using a 3:1 pentane/toluene (5 mL) solution and filtered through a silica plug. Volatiles were removed under vacuum to give **4** (79.0 mg, 83%) as a pale yellow solid. <sup>1</sup>H and <sup>13</sup>C NMR data were consistent with those that have been previously reported.<sup>30</sup>

( $\mu$ -Crotyl)( $\mu$ -Cl)Pd<sub>2</sub>(IPr)<sub>2</sub> (**5**). Pd( $\eta^3$ -crotyl)(IPr)Cl (**2**) (75.0 mg, 0.128 mmol) and potassium carbonate (27 mg, 1.5 equiv) were transferred to a Schlenk flask and placed under dinitrogen. Degassed ethanol (5 mL) was transferred by cannula into the Schlenk flask at rt, and the reaction mixture was stirred at 40 °C for 3 h. Volatiles were removed under vacuum. The residue was extracted using a 3:1 pentane/toluene (5 mL) solution and filtered through a silica plug. Volatiles were removed under vacuum to give **5** (60.4 mg, 87%) as a yellow solid, which contained a 9:1 mixture of *anti* and *syn* isomers. Redissolving the mixture in C<sub>6</sub>H<sub>6</sub> and leaving it to stand for 12 h at room temperature allowed for isolation of only the *anti* isomer of **5**. Crystals for X-ray analysis were grown through slow evaporation of a saturated solution in pentane/toluene. Anal. Calcd for C<sub>58</sub>H<sub>79</sub>ClN<sub>4</sub>Pd<sub>2</sub>: C, 64.47; H, 7.37; N, 5.18. Found: C, 64.38; H, 7.39; N, 5.20.

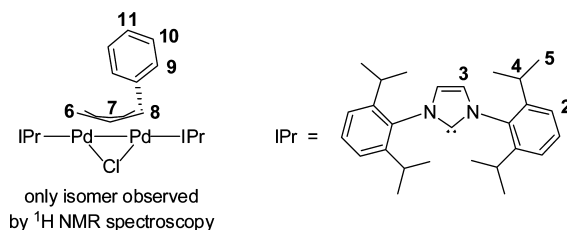
*Anti* isomer (major product, geometry determined by irradiating the central proton signal at  $\delta$  1.68 in a 1D NOESY experiment): <sup>1</sup>H NMR (400 MHz, C<sub>6</sub>D<sub>6</sub>) 7.22 (m, 4H, H1), 7.15–7.07 (m, 8H, H2), 6.64 (s, 2H, H3), 6.63 (s, 2H, H3), 3.22 (septet,  $J = 6.8$  Hz, 2H, H4), 3.17



(septet,  $J = 6.8$  Hz, 2H, H4), 3.14–3.04 (m, 5H, H4 and H8), 1.91 (dd,  $J = 8.3, 2.1$  Hz, 1H, H6-*syn*), 1.68 (m, 1H, H7), 1.37 (d,  $J = 6.8$  Hz, 6H, H5), 1.34 (d,  $J = 6.8$  Hz, 6H, H5), 1.31 (d,  $J = 6.8$  Hz, 6H, H5), 1.26 (d,  $J = 6.8$  Hz, 6H, H5), 1.13 (d,  $J = 6.8$  Hz, 6H, H5), 1.12 (s,  $J = 6.4$  Hz, 6H, H5), 1.10 (d,  $J = 6.6$  Hz, 6H, H5), 1.08 (d,  $J = 6.9$  Hz, 6H, H5), 0.85 (dd,  $J = 12.3, 2.2$  Hz, 1H, H6-*anti*), 0.24 (d,  $J = 6.2$  Hz, 3H, H9). <sup>13</sup>C{<sup>1</sup>H} NMR (126 MHz, C<sub>6</sub>D<sub>6</sub>) 192.36, 191.91, 146.02, 146.01, 145.96, 145.90, 137.26, 137.20, 128.85, 128.83, 123.45, 123.33, 123.33, 123.29, 122.28, 122.13, 55.07, 36.45, 28.49, 28.45, 28.36, 25.58, 25.27, 25.24, 23.32, 23.16, 23.14, 23.08, 20.12, 15.21.

*Syn* isomer (minor product): Some unobserved peaks are visible in the <sup>1</sup>H NMR spectrum. <sup>1</sup>H NMR (400 MHz, C<sub>6</sub>D<sub>6</sub>) 6.65 (s, 2H, H3), 6.59 (s, 2H, H3), 2.23 (dd,  $J = 8.0, 1.9$  Hz, 1H, H6-*syn*), 0.44 (dd,  $J = 12.1, 1.9$  Hz, 1H, H6-*anti*).

( $\mu$ -Cinnamyl)( $\mu$ -Cl)Pd<sub>2</sub>(IPr)<sub>2</sub> (**6**). Pd( $\eta^3$ -cinnamyl)(IPr)Cl (**3**) (119.5 mg, 0.185 mmol) and potassium carbonate (127 mg, 5 equiv) were transferred to a Schlenk flask and placed under dinitrogen. Degassed ethanol (5 mL) was transferred by cannula into the Schlenk flask at rt, and the reaction mixture was stirred at 40 °C for 3 h. Volatiles were removed under vacuum. The residue was extracted using toluene (5 mL) and filtered using a cannula. Volatiles were then removed under vacuum, and the remaining residue was washed with pentane (3  $\times$  2 mL) and dried to give **6** (87.2 mg, 83%) as a yellow solid. Crystals for X-ray analysis were grown by layering MeOH over a concentrated solution of **6** in THF. Anal. Calcd for C<sub>63</sub>H<sub>81</sub>ClN<sub>4</sub>Pd<sub>2</sub>: C, 66.22; H, 7.15; N, 4.90. Found: C, 66.34; H, 7.29; N, 4.84.



<sup>1</sup>H NMR (500 MHz, C<sub>6</sub>D<sub>6</sub>, geometry determined by irradiating the central proton signal at  $\delta$  1.75 in a 1D NOESY experiment) 7.28–7.19 (m, 4H, H1), 7.13 (d,  $J = 8.0$  Hz, 4H, H2), 7.09 (d,  $J = 7.7$  Hz, 2H, H2), 7.04 (d,  $J = 7.6$  Hz, 2H, H2), 6.91 (t,  $J = 7.8$  Hz, 1H, H11), 6.76 (t,  $J = 7.6$  Hz, 2H, H10), 6.62 (s, 2H, H3), 6.62 (s, 2H, H3), 6.54 (d,  $J = 7.3$  Hz, 2H, H9), 3.86 (d,  $J = 8.2$  Hz, 1H, H8), 3.21 (septet,  $J = 6.9$  Hz, 2H, H4), 3.16–3.06 (m, 4H, H4), 3.01 (septet,  $J = 7.0$  Hz, 2H), 1.87 (dd,  $J = 8.8, 1.5$  Hz, 1H, H6-*syn*), 1.75 (m, 1H, H7), 1.37 (d,  $J = 6.8$  Hz, 6H, H5), 1.30 (d,  $J = 6.8$  Hz, 6H, H5), 1.26 (d,  $J = 6.8$  Hz, 6H, H5), 1.10 (m, 18H, H5), 0.98 (d,  $J = 6.9$  Hz, 6H, H5), 0.94 (d,  $J = 6.7$  Hz, 6H, H5), 0.67 (dd,  $J = 12.3, 1.8$  Hz, 1H, H6-*anti*). <sup>13</sup>C{<sup>1</sup>H} NMR (126 MHz, C<sub>6</sub>D<sub>6</sub>) 192.29, 191.12, 146.54, 146.24, 146.09, 144.48, 137.95, 137.54, 129.90, 129.38, 129.24, 126.81, 123.82, 123.76, 123.72, 123.66, 123.34, 122.92, 122.69, 51.69, 44.50, 28.91, 28.90, 28.88, 28.78, 25.94, 25.93, 25.65, 25.53, 23.50, 23.44, 23.37, 22.78, 21.06. One of the <sup>13</sup>C peaks in the aromatic region was obscured by solvent.

**Suzuki–Miyaura Cross-Coupling Reactions, General Procedures.** Tables 1 and 4. Each reaction was performed under dinitrogen in a 1 dram vial containing a flea stir bar and sealed with a septum cap. To each vial was added 800  $\mu$ L of an <sup>i</sup>PrOH stock solution (0.625 M 4-chlorotoluene, 0.6875 M KO<sup>t</sup>Bu, 0.3125 M naphthalene) and 150  $\mu$ L of a MeOH stock solution (3.5 M phenylboronic acid). Each vial was then heated using an aluminum block heater set to the appropriate temperature. After thermal equilibration, each reaction was initiated via addition of 50  $\mu$ L of the appropriate precatalyst solution in THF (0.1 M [Pd]<sub>tot</sub> for Table 1, 0.2 M [Pd]<sub>tot</sub> for Table 4). Aliquots ( $\sim$ 50–100  $\mu$ L) were removed at reaction times of 30 and 60 min. Aliquots were

purified by filtration through pipet filters containing approximately 1 cm of silica and eluted with 1–1.2 mL of ethyl acetate directly into GC vials. Conversion was determined by comparison of the GC responses of product and the internal naphthalene standard.

**Table 5.** Potassium carbonate (0.75 mmol) or potassium phosphate (0.75 mmol) was transferred on the benchtop into a 1 dram vial containing a flea stir bar. The vial was sealed with a septum cap and placed under dinitrogen (by cycling three times between vacuum and dinitrogen) on a Schlenk line through a needle. To each vial was added 950  $\mu\text{L}$  of an EtOH or  $^i\text{PrOH}$  stock solution (0.526 M 4-chlorotoluene, 0.553 M phenylboronic acid, 0.263 M naphthalene). Each vial was then heated using an aluminum block heater set to 25 or 40  $^\circ\text{C}$ . After thermal equilibration, each reaction was initiated via addition of 50  $\mu\text{L}$  of a 0.1 M solution of the precatalyst in THF. Aliquots ( $\sim 50$ – $100 \mu\text{L}$ ) were removed at reaction times of 30 and 60 min. Aliquots were purified by filtration through pipet filters containing approximately 1 cm of silica and eluted with 1–1.2 mL of ethyl acetate directly into GC vials. Conversion was determined by comparison of the GC responses of product and the internal naphthalene standard.

## ■ ASSOCIATED CONTENT

### ● Supporting Information

Further experimental details including (i) procedures for reactions investigating activation of **1**–**3** and synthesis of dimers in different solvents, (ii) protocols for observing and quantifying the presence of dimers **4**–**6** under catalytic conditions, (iii) procedures for investigating disproportionation and comproportionation reactions involving **1**–**6**, and (iv) X-ray crystallographic information for **5** and **6**; computational details including (i) optimized coordinates and energies, (ii) a comparison of experimental and calculated bond lengths and distances, (iii) test calculations performed using the full IPr ligand, and (iv) information about alternative mechanisms. This material is available free of charge via the Internet at <http://pubs.acs.org>.

## ■ AUTHOR INFORMATION

### Corresponding Authors

david.balcells@kjemi.uio.no

nilay.hazari@yale.edu

### Notes

The authors declare no competing financial interest.

## ■ ACKNOWLEDGMENTS

N.H. gratefully acknowledges support through a Doctoral New Investigator Grant from the ACS Petroleum Research Fund (51009-DNI3). D.B. and M.T. acknowledge support from the Norwegian Research Council through the Center of Excellence for Theoretical and Computational Chemistry (CTCC) (Grant No. 179568/V30) and the Norwegian Metacenter for Computational Science (NOTUR; Grant nn4654k). D.P.H. thanks the NSF for support both through the Nordic Research Opportunity and as an NSF Graduate Research Fellow. D.P.H. also acknowledges the Norwegian Research Council for a mobility grant (Grant No. 220360/F11). We are grateful to Dr. Paul Anastas' group for use of their GC instrument.

## ■ REFERENCES

(1) (a) Hartwig, J. F. *Acc. Chem. Res.* **2008**, *41*, 1534. (b) Martin, R.; Buchwald, S. L. *Acc. Chem. Res.* **2008**, *41*, 1461. (c) Marion, N.; Nolan, S. P. *Acc. Chem. Res.* **2008**, *41*, 1440. (d) Fu, G. C. *Acc. Chem. Res.* **2008**, *41*, 1555. (e) Würtz, S.; Glorius, F. *Acc. Chem. Res.* **2008**, *41*, 1523. (f) Magano, J.; Dunetz, J. R. *Chem. Rev.* **2011**, *111*, 2177. (g) Li, H.; Johansson Seechurn, C. C. C.; Colacot, T. J. *ACS Catal.* **2012**, *2*,

1147. (h) Johansson Seechurn, C. C. C.; Kitching, M. O.; Colacot, T. J.; Snieckus, V. *Angew. Chem., Int. Ed.* **2012**, *51*, 5062. (i) Valente, C.; Calimsiz, S.; Hoi, K. H.; Mallik, D.; Sayah, M.; Organ, M. G. *Angew. Chem., Int. Ed.* **2012**, *51*, 3314.

(2) (a) Littke, A. F.; Fu, G. C. *Angew. Chem., Int. Ed.* **1999**, *38*, 2411. (b) Littke, A. F.; Dai, C.; Fu, G. C. *J. Am. Chem. Soc.* **2000**, *122*, 4020.

(3) (a) Wolfe, J. P.; Singer, R. A.; Yang, B. H.; Buchwald, S. L. *J. Am. Chem. Soc.* **1999**, *121*, 9550. (b) Aranyos, A.; Old, D. W.; Kiyomori, A.; Wolfe, J. P.; Sadighi, J. P.; Buchwald, S. L. *J. Am. Chem. Soc.* **1999**, *121*, 4369. (c) Wolfe, J. P.; Buchwald, S. L. *Angew. Chem., Int. Ed.* **1999**, *38*, 2413.

(4) (a) Shelby, Q.; Kataoka, N.; Mann, G.; Hartwig, J. J. *Am. Chem. Soc.* **2000**, *122*, 10718. (b) Kataoka, N.; Shelby, Q.; Stambuli, J. P.; Hartwig, J. F. *J. Org. Chem.* **2002**, *67*, 5553.

(5) (a) Lundgren, R. J.; Hesp, K. D.; Stradiotto, M. *Synlett* **2011**, 2443. (b) Lundgren, R. J.; Stradiotto, M. *Chem.—Eur. J.* **2012**, *18*, 9758.

(6) Christmann, U.; Vilar, R. *Angew. Chem., Int. Ed.* **2005**, *44*, 366.

(7) (a) Biscoe, M. R.; Fors, B. P.; Buchwald, S. L. *J. Am. Chem. Soc.* **2008**, *130*, 6686. (b) Kinzel, T.; Zhang, Y.; Buchwald, S. L. *J. Am. Chem. Soc.* **2010**, *132*, 14073. (c) Bruno, N. C.; Tudge, M. T.; Buchwald, S. L. *Chem. Sci.* **2013**, *4*, 916.

(8) (a) O'Brien, C. J.; Kantchev, E. A. B.; Valente, C.; Hadei, N.; Chass, G. A.; Lough, A.; Hopkinson, A. C.; Organ, M. G. *Chem.—Eur. J.* **2006**, *12*, 4743. (b) Organ, M. G.; Chass, G. A.; Fang, D.-C.; Hopkinson, A. C.; Valente, C. *Synthesis* **2008**, 2776. (c) Nasielski, J.; Hadei, N.; Achonduh, G.; Kantchev, E. A. B.; O'Brien, C. J.; Lough, A.; Organ, M. G. *Chem.—Eur. J.* **2010**, *16*, 10844.

(9) (a) Viciu, M. S.; Germaneau, R. F.; Nolan, S. P. *Org. Lett.* **2002**, *4*, 4053. (b) Viciu, M. S.; Germaneau, R. F.; Navarro-Fernandez, O.; Stevens, E. D.; Nolan, S. P. *Organometallics* **2002**, *21*, 5470. (c) Navarro, O.; Kaur, H.; Mahjoor, P.; Nolan, S. P. *J. Org. Chem.* **2004**, *69*, 3173. (d) Marion, N.; Navarro, O.; Mei, J.; Stevens, E. D.; Scott, N. M.; Nolan, S. P. *J. Am. Chem. Soc.* **2006**, *128*, 4101.

(10) (a) Nasielski, J.; Hadei, N.; Achonduh, G.; Kantchev, E. A. B.; O'Brien, C. J.; Lough, A.; Organ, M. G. *Chem.—Eur. J.* **2012**, *16*, 10844. (b) Sayah, M.; Lough, A. J.; Organ, M. G. *Chem.—Eur. J.* **2013**, *19*, 2749.

(11) (a) Hill, L. L.; Crowell, J. L.; Tutwiler, S. L.; Massie, N. L.; Hines, C. C.; Griffin, S. T.; Rogers, R. D.; Shaughnessy, K. H.; Grasa, G. A.; Johansson Seechurn, C. C. C.; Li, H.; Colacot, T. J.; Chou, J.; Woltermann, C. J. *J. Org. Chem.* **2010**, *75*, 6477. (b) Johansson Seechurn, C. C. C.; Parisel, S. L.; Colacot, T. J. *J. Org. Chem.* **2011**, *76*, 7918.

(12) (a) Werner, H. *Adv. Organomet. Chem.* **1981**, *19*, 155. (b) Murahashi, T.; Kurosawa, H. *Coord. Chem. Rev.* **2002**, *231*, 207. (c) Hazari, N.; Hruszkewycz, D. P.; Wu, J. *Synlett* **2011**, 1793.

(13) (a) Egbert, J. D.; Chartoire, A.; Slawin, A. M. Z.; Nolan, S. P. *Organometallics* **2011**, *30*, 4494. (b) Fantasia, S.; Nolan, S. P. *Chem.—Eur. J.* **2008**, *14*, 6987. (c) Denmark, S. E.; Smith, R. C. *Synlett* **2006**, 18, 2921. (d) Ortiz, D.; Blug, M.; Goff, X.-F. L.; Floch, P. L.; Mezaillas, N.; Maitre, P. *Organometallics* **2012**, *31*, 5975. (e) Alsabeh, P. G.; Lundgren, R. J.; McDonald, R.; Johansson Seechurn, C. C. C.; Colacot, T. J.; Stradiotto, M. *Chem.—Eur. J.* **2013**, *19*, 2131.

(14) Colacot and co-workers briefly speculated about the role of  $\text{Pd}^{\text{I}}$   $\mu$ -allyl dimers when monomeric  $\eta^3$ -allyl Pd complexes are used as precatalysts in ref 11a. They also conducted some interesting preliminary mechanistic studies, which imply the intermediacy of  $\text{Pd}^{\text{I}}$   $\mu$ -allyl dimers in catalysis in ref 11b. These two studies served as a large inspiration for the current study.

(15) Monomeric Pd complexes with substituents in the 2-position of the allyl ligand have also been reported in the literature, but only complexes with 2-methylallyl substituents have been explored as precatalysts for cross-coupling: (a) ref 11b. (b) Cawley, M. J.; Cloke, F. G. N.; Fitzmaurice, R. J.; Pearson, S. E.; Scott, J. S.; Caddick, S. *Org. Biomol. Chem.* **2008**, *6*, 2820. (c) Navarro, O.; Oonishi, Y.; Kelly, R. A.; Stevens, E. D.; Briel, O.; Nolan, S. P. *J. Organomet. Chem.* **2004**, 689, 3722. In these reports, the 2-methylallyl-supported precatalysts displayed similar catalytic efficiency to the corresponding unsub-

stituted allyl precatalysts. Overall, at this stage the effect of substituents in the 2-position in precatalysts of the type Pd(L)( $\eta^3$ -allyl)Cl has not been evaluated in detail and is a topic that is currently being explored in our laboratory.

(16) Cinnamyl-supported **3** and its SIPr analogue were used as precatalysts in the following reports: (a) Navarro, O.; Marion, N.; Mei, J.; Nolan, S. P. *Chem.—Eur. J.* **2006**, *12*, 5142. (b) Lipshutz, B. H.; Petersen, T. B.; Abela, A. R. *Org. Lett.* **2008**, *10*, 1333. (c) Berini, C.; Brayton, D. F.; Mocka, C.; Navarro, O. *Org. Lett.* **2009**, *11*, 4244. (d) Prasad, B. A. B.; Buechele, A. E.; Gilbertson, S. R. *Org. Lett.* **2010**, *12*, 5422. (e) Woodmansee, D. H.; Mueller, M.-A.; Neuburger, M.; Pfaltz, A. *Chem. Sci.* **2010**, *1*, 72. (f) Landers, B.; Berini, C.; Wang, C.; Navarro, O. *J. Org. Chem.* **2011**, *76*, 1390.

(17) For select examples of the use of cinnamyl-supported precatalysts using other ligands, see: (a) Luan, X.; Mariz, R.; Robert, C.; Gatti, M.; Blumentritt, S.; Linden, A.; Dorta, R. *Org. Lett.* **2008**, *10*, 5569. (b) Schoeps, D.; Sashuk, V.; Ebert, K.; Plenio, H. *Organometallics* **2009**, *28*, 3922. (c) Vieille-Petit, L.; Luan, X.; Mariz, R.; Blumentritt, S.; Linden, A.; Dorta, R. *Eur. J. Inorg. Chem.* **2009**, 1861. (d) Luan, X.; Wu, L.; Drinkel, E.; Mariz, R.; Gatti, M.; Dorta, R. *Org. Lett.* **2010**, *12*, 1912. (e) Wu, L.; Drinkel, E.; Gaggia, F.; Capolicchio, S.; Linden, A.; Falivene, L.; Cavallo, L.; Dorta, R. *Chem.—Eur. J.* **2011**, *17*, 12886. (f) Chartoire, A.; Lesieur, M.; Falivene, L.; Slawin, A. M. Z.; Cavallo, L.; Cazin, C. S. J.; Nolan, S. P. *Chem.—Eur. J.* **2012**, *18*, 4517. (g) Terashima, T.; Inomata, S.; Ogata, K.; Fukuzawa, S.-i. *Eur. J. Inorg. Chem.* **2012**, *2012*, 1387. (h) Wu, L.; Falivene, L.; Drinkel, E.; Grant, S.; Linden, A.; Cavallo, L.; Dorta, R. *Angew. Chem., Int. Ed.* **2012**, *51*, 2870. (i) Wheaton, C. A.; Bow, J.-P. J.; Stradiotto, M. *Organometallics* **2013**, *32*, 6148.

(18) The chloride-bridged dimeric precursor to the cinnamyl-supported precatalysts was demonstrated to be a superior Pd source compared to other common Pd sources in the following reports: (a) Martin, R.; Buchwald, S. L. *Org. Lett.* **2008**, *10*, 4561. (b) Lundgren, R. J.; Stradiotto, M. *Angew. Chem., Int. Ed.* **2010**, *49*, 8686. (c) Lundgren, R. J.; Sapping-Kumankumah, A.; Stradiotto, M. *Chem.—Eur. J.* **2010**, *16*, 1983. (d) Rousseaux, S.; Garcia-Fortanet, J.; Del Aguila Sanchez, M. A.; Buchwald, S. L. *J. Am. Chem. Soc.* **2011**, *133*, 9282. (e) Hermange, P.; Gøgsig, T. M.; Lindhardt, A. T.; Taaning, R. H.; Skrydstrup, T. *Org. Lett.* **2011**, *13*, 2444. (f) Hesp, K. D.; Lundgren, R. J.; Stradiotto, M. *J. Am. Chem. Soc.* **2011**, *133*, 5194. (g) Gøgsig, T. M.; Nielsen, D. U.; Lindhardt, A. T.; Skrydstrup, T. *Org. Lett.* **2012**, *14*, 2536. (h) Schranck, J.; Tlili, A.; Neumann, H.; Alsalbeh, P. G.; Stradiotto, M.; Beller, M. *Chem.—Eur. J.* **2012**, *18*, 15592. (i) Salvi, L.; Davis, N. R.; Ali, S. Z.; Buchwald, S. L. *Org. Lett.* **2012**, *14*, 170.

(19) Weissman, H.; Shimon, L. J. W.; Milstein, D. *Organometallics* **2004**, *23*, 3931.

(20) (a) Yamamoto, T.; Saito, O.; Yamamoto, A. *J. Am. Chem. Soc.* **1981**, *103*, 5600. (b) Yamamoto, T.; Akimoto, M.; Saito, O.; Yamamoto, A. *Organometallics* **1986**, *5*, 1559. (c) Portnoy, M.; Frolow, F.; Milstein, D. *Organometallics* **1991**, *10*, 3960. (d) Tromp, M.; Sietsma, J. R. A.; van Bokhoven, J. A.; van Strijdonck, G. P. F.; van Haaren, R. J.; van der Eerden, A. M. J.; van Leeuwen, P. W. N. M.; Koningsberger, D. C. *Chem. Commun.* **2003**, 128. (e) Markert, C.; Neuburger, M.; Kulicke, K.; Meuwly, M.; Pfaltz, A. *Angew. Chem., Int. Ed.* **2007**, *46*, 5892. (f) Baya, M.; Houghton, J.; Konya, D.; Champouret, Y.; Daran, J.-C.; Almeida, L. K. Q.; Schoon, L.; Mul, W. P.; van Oort, A. B.; Meijboom, N.; Drent, E.; Orpen, A. G.; Poli, R. *J. Am. Chem. Soc.* **2008**, *130*, 10612. (g) Ragaini, F.; Larici, H.; Rimoldi, M.; Caselli, A.; Ferretti, F.; Macchi, P.; Casati, N. *Organometallics* **2011**, *30*, 2385. (h) Agrawal, D.; Schroder, D.; Frech, C. M. *Organometallics* **2011**, *30*, 3579. (i) Boyd, P. D. W.; Edwards, A. J.; Gardiner, M. G.; Ho, C. C.; Lemee-Cailleau, M.-H.; McGuinness, D. S.; Riapanitra, A.; Steed, J. W.; Stringer, D. N.; Yates, B. F. *Angew. Chem., Int. Ed.* **2010**, *49*, 6315. (j) Bedford, R. B.; Haddow, M. F.; Mitchell, C. J.; Webster, R. L. *Angew. Chem., Int. Ed.* **2011**, *50*, 5524. (k) Aufiero, M.; Proutiere, F.; Schoenebeck, F. *Angew. Chem., Int. Ed.* **2012**, *51*, 7226.

(21) (a) Vilar, R.; Mingos, D. M. P.; Cardin, C. J. *J. Chem. Soc., Dalton Trans.* **1996**, 4313. (b) Stambuli, J. P.; Kuwano, R.; Hartwig, J. F. *Angew. Chem., Int. Ed.* **2002**, *41*, 4746. (c) Christmann, U.; Vilar, R.; White, A. J. P.; Williams, D. J. *Chem. Commun.* **2004**, 1294. (d) Barder, T. E. *J. Am. Chem. Soc.* **2006**, *128*, 898. (e) Han, X.; Weng, Z.; Hor, T. S. A. *J. Organomet. Chem.* **2007**, *692*, S690. (f) Das, R. K.; Saha, B.; Rahaman, S. M. W.; Bera, J. K. *Chem.—Eur. J.* **2010**, *16*, 14459.

(22) (a) Elliott, E. L.; Ray, C. R.; Kraft, S.; Atkins, J. R.; Moore, J. S. *J. Org. Chem.* **2006**, *71*, S282. (b) Finke, A. D.; Elleby, E. C.; Boyd, M. J.; Weissman, H.; Moore, J. S. *J. Org. Chem.* **2009**, *74*, 8897. (c) Denmark, S. E.; Baird, J. D. *Org. Lett.* **2006**, *8*, 793. (d) Denmark, S. E.; Baird, J. D.; Regens, C. S. *J. Org. Chem.* **2008**, *73*, 1440.

(23) (a) Christmann, U.; Pantazis, D. A.; Benet-Buchholz, J.; McGrady, J. E.; Maseras, F.; Vilar, R. *Organometallics* **2006**, *25*, S990. (b) Christmann, U.; Pantazis, D. A.; Benet-Buchholz, J.; McGrady, J. E.; Maseras, F.; Vilar, R. *J. Am. Chem. Soc.* **2006**, *128*, 6376. (c) Jimeno, C.; Christmann, U.; Escudero-Adan, E. C.; Vilar, R.; Pericas, M. A. *Chem.—Eur. J.* **2012**, *18*, 16510. (d) Proutiere, F.; Aufiero, M.; Schoenebeck, F. *J. Am. Chem. Soc.* **2012**, *134*, 606.

(24) See Supporting Information for more details.

(25) (a) Osakada, K.; Chiba, T.; Nakamura, Y.; Yamamoto, T.; Yamamoto, A. *Organometallics* **1989**, *8*, 2602. (b) Kurosawa, H.; Hirako, K.; Natsume, S.; Ogoshi, S.; Kanehisa, N.; Kai, Y.; Sakaki, S.; Takeuchi, K. *Organometallics* **1996**, *15*, 2089.

(26) Sakaki, S.; Takeuchi, K.; Sugimoto, M.; Kurosawa, H. *Organometallics* **1997**, *16*, 2995.

(27) Hruszkewycz, D. P.; Wu, J.; Green, J. C.; Hazari, N.; Schmeier, T. J. *Organometallics* **2012**, *31*, 470.

(28) In support of our proposal that the Pd–C bond distances to the terminal carbon atoms of the  $\mu$ -allyl ligand are inequivalent, the DFT-optimized structures of **5** and **6** have different Pd–C bond distances. See the Supporting Information for more information.

(29) Crabtree, R. H. *The Organometallic Chemistry of the Transition Metals*, 5th ed.; Wiley: New York, 2009.

(30) Hruszkewycz, D. P.; Wu, J.; Hazari, N.; Incarvito, C. D. *J. Am. Chem. Soc.* **2011**, *133*, 3280.

(31) For a similar mechanism of activation that involves the isopropoxide anion, see ref 13b.

(32) Dible, B. R.; Cowley, R. E.; Holland, P. L. *Organometallics* **2011**, *30*, 5123.

(33) In ref 32 a very dilute ( $\sim 0.1$  M) solution of substrates in  $^i$ PrOH (no MeOH cosolvent) and precatalyst in THF was utilized. We added MeOH as a cosolvent in order to perform our reactions at higher concentration.

(34) Krause, J.; Cestarc, G.; Haack, K.-J.; Seevogel, K.; Storm, W.; Pörschke, K.-R. *J. Am. Chem. Soc.* **1999**, *121*, 9807.

(35) For related cross-over experiments, see ref 25b.

(36) Given the extremely large size of the IPr ligand, it was not possible to run a full series of calculations with the complete experimental systems. A limited number of calculations with the IPr ligand are described in the Supporting Information.

(37) Faller, J. W.; Thomsen, M. E.; Mattina, M. J. *J. Am. Chem. Soc.* **1971**, *93*, 2642.

(38) In the trapping experiments, products with  $^1$ H NMR chemical shifts that are consistent with those expected for the *anti* isomer of complexes of the type Pd(IPr)( $\eta^3$ -allyl)Cl were observed on some occasions. However, these peaks rapidly decreased in intensity, while peaks associated with the *syn* isomers of complexes of the type Pd(IPr)( $\eta^3$ -allyl)Cl increased. Therefore, no attempts were made to characterize the putative *anti* isomers.

(39) The loading of the weak base in these reactions is similar to that described by Organ and co-workers in ref 8a, which reports a family of highly active precatalysts for the Suzuki–Miyaura coupling with weak base. Our precatalyst system seems to be slightly more active than the precatalysts described in ref 8a, although there are differences in the exact reaction conditions, which make direct comparison difficult.

(40) Genov, M.; Almorin, A.; Espinet, P. *Chem.—Eur. J.* **2006**, *12*, 9346.

(41) (a) Arduengo, A. J., III; Krafczyk, R.; Schmutzler, R.; Craig, H. A.; Goerlich, J. R.; Marshall, W. J.; Unverzagt, M. *Tetrahedron* **1999**, *55*, 14523. (b) Tang, P.; Wang, W.; Ritter, T. *J. Am. Chem. Soc.* **2011**, *133*, 11482.

(42) Dolomanov, O. V.; Bourhis, L. J.; Gildea, R. J.; Howard, J. A. K.; Puschmann, H. *J. Appl. Crystallogr.* **2009**, *42*, 339.

(43) Sheldrick, G. *Acta Crystallogr., Sect. A: Found. Crystallogr.* **2008**, *64*, 112.

(44) Frisch, M. J.; Trucks, G. W.; Schlegel, H. B.; Scuseria, G. E.; Robb, M. A.; Cheeseman, J. R.; Scalmani, G.; Barone, V.; Mennucci, B.; Petersson, G. A.; Nakatsuji, H.; Caricato, M.; Li, X.; Hratchian, H. P.; Izmaylov, A. F.; Bloino, J.; Zheng, G.; Sonnenberg, J. L.; Hada, M.; Ehara, M.; Toyota, K.; Fukuda, R.; Hasegawa, J.; Ishida, M.; Nakajima, T.; Honda, Y.; Kitao, O.; Nakai, H.; Vreven, T.; Montgomery, J. A.; Peralta, J. E.; Ogliaro, F.; Bearpark, M.; Heyd, J. J.; Brothers, E.; Kudin, K. N.; Staroverov, V. N.; Keith, T.; Kobayashi, R.; Normand, J.; Raghavachari, K.; Rendell, A.; Burant, J. C.; Iyengar, S. S.; Tomasi, J.; Cossi, M.; Rega, N.; Millam, J. M.; Klene, M.; Knox, J. E.; Cross, J. B.; Bakken, V.; Adamo, C.; Jaramillo, J.; Gomperts, R.; Stratmann, R. E.; Yazyev, O.; Austin, A. J.; Cammi, R.; Pomelli, C.; Ochterski, J. W.; Martin, R. L.; Morokuma, K.; Zakrzewski, V. G.; Voth, G. A.; Salvador, P.; Dannenberg, J. J.; Dapprich, S.; Daniels, A. D.; Farkas, O.; Foresman, J. B.; Ortiz, J. V.; Cioslowski, J.; Fox, D. J. *Gaussian09*; Gaussian, Inc.: Wallingford, CT, 2013.

(45) Hehre, W. J.; Ditchfield, R.; Pople, J. A. *J. Chem. Phys.* **1972**, *56*, 2257.

(46) (a) Bergner, A.; Dolg, M.; Küchle, W.; Stoll, H.; Preuss, H. *Mol. Phys.* **1993**, *80*, 1431. (b) Peterson, K. A.; Figgen, D.; Dolg, M.; Stoll, H. *J. Chem. Phys.* **2007**, *126*, 124101.

(47) (a) Zhao, Y.; Truhlar, D. G. *Theor. Chem. Acc.* **2008**, *120*, 215. (b) Zhao, Y.; Truhlar, D. G. *Acc. Chem. Res.* **2008**, *41*, 157.

(48) Marenich, A. V.; Cramer, C. J.; Truhlar, D. G. *J. Phys. Chem. B* **2009**, *113*, 6378.

(49) Krishnan, R.; Binkley, J. S.; Seeger, R.; Pople, J. A. *J. Chem. Phys.* **1980**, *72*, 650.